EMBRY-RIDDLE
Aeronautical University™
SCHOLARLY COMMONS

Publications

8-20-1981

Characteristics of Water Vapor Tracked Winds

Frederick R. Mosher
University of Wisconsin-Madison, moshe774@erau.edu

Follow this and additional works at: https://commons.erau.edu/publication

Part of the Meteorology Commons

Characteristics of Water Vapor Tracked Winds

by
Frederick R. Mosher
Tod Stewart

August 20, 1981

Space Science and Engineering Center
at the University of Wisconsin-Madison
1225 West Dayton St.
Madison, Wisconsin 53706

Final Report for ONR Contract N00014-80-C-0632

REPORT DOCUMENTATION PAGE		READ INSTRUCTIONS BEFORE COMPLETING FORM
1. REPORT NUMBER	2. GOVT ACCESSION NO.	3. RECIPIENT'S CATALOG NUMBER
4. TITLE (and Subtitle) Characteristics of Water Vapor Tracked Winds		5. TYPE OF REPORT & PERIOD COVERED Final Report
		6. PERFORMING ORG. REPORT NUMBER
7. AUTHOR(s) Frederick R. Mosher Tod Stewart		8. CONTRACT OR GRANT NUMBER(s) N00014-80-C-0632
9. PERFORMING ORGANIZATION NAME AND ADDRESS Space Science and Engineering Center at the University of Wisconsin-Madison 1225 West Dayton St., Madison, WI 53706		10. PROGRAM ELEMENT, PROJECT, TASK AREA & WORK UNIT NUMBERS Program Element 62759N Project 9F52551792
11. CONTROLLING OFFICE NAME AND ADDRESS Naval Environmental Prediction Research Facility Monterey, California 93940		12. REPORT DATE August 20, 1981
		13. NUMBER OF PAGES 50
14. MONITORING AGENCY NAME & ADDRESS(if different from Controlling Office) same		15. SECURITY CLASS. (of this report) Unclassified
		15a. DECLASSIFICATION/DOWNGRADING SCHEDULE

16. DISTRIBUTION STATEMENT (of this Report)

Approved for public release; Distribution unlimited.

17. DISTRIBUTION STATEMENT (of the abstract entered in Block 20, if different from Report)

18. SUPPLEMENTARY NOTES

19. KEY WORDS (Continue on reverse side if necessary and identify by block number)

Water Vapor Winds	VAS
Cloud Winds	METEOSAT
Meteorological Satellite Measurements	Remote Sensing of Winds

20. ABSTRACT (Continue on reverse side if necessary and identify by block number)

Wind measurements were obtained by tracking water vapor features on Meteosat and GOES-VAS 6.7 micron water vapor images. While pure water vapor features are fuzzy, there are discernible features which can be tracked. An investigation of preprocessing algorithms designed to bring out the features to be tracked showed that high pass filters tended to bring out the noise in the image, while low pass filters washed out the features. Equal population gray scale stretching enhanced both the water

DD FORM 1473 EDITION OF 1 NOV 65 IS OBSOLETE
1 JAN 73
S/N 0102-LF-014-6601

Abstract

Wind measurements were obtained by tracking water vapor features on Meteosat and GOES-VAS 6.7 micron water vapor images. While pure water vapor features are fuzzy, there are discernible features which can be tracked. An investigation of preprocessing algorithms designed to bring out the features to be tracked showed that high pass filters tended to bring out the noise in the image, while low pass filters washed out the features. Equal population gray scale stretching enhanced both the water vapor features and the cloud features. Sliced linear gray scale stretching under operator control gave the best enhancement to the water vapor features. The height assignment of water vapor features is uncertain. The feature is in the middle troposphere, but can vary between 300 mb and 700 mb. Rather than assign all the winds at an arbitrary height, an attempt was made to infer the water vapor height from the cloud heights and motions as compared to the water vapor motions.

Water vapor tracking was done interactively using the Man-computer Interactive Data Access System (McIDAS). While correlation tracking was attempted, it was successful in only 10% of the measurements. Manual tracking was used for the rest. A study to determine the optimal time interval for tracking fuzzy water vapor features found that a total tracking time of two to four hours produced the best results. The higher spatial resolution of the Meteosat's sensor made it possible to track more features than with the VAS instrument.

Analysis of the derived wind fields showed that water vapor does provide additional meteorological information around jets and mid-troposphere motions not normally provided by cloud drift winds. Comparisons with radiosonde and cloud winds showed the water vapor winds to have a slightly lower quality

then cloud winds. Errors tended to be about 2n/sec worse than cloud tracked

wind errors. This is probably due to the difficulty in tracking the fuzzy

water vapor features and the uncertainties of height assignments.

I. Introduction

    The purpose of this study was to determine the validity and particular characteristics of water vapor tracked winds. The use of space-based observing platforms has resulted in a tremendous increase in meteorological data. Possibly the most significant data derived from satellites are the cloud tracked winds obtained from geostationary visible and infrared images. These measurements provide wind information in otherwise data sparse or data void regions of the globe.

    Cloud motion vectors, however, are limited by the existence of traceable clouds. No measurements are possible in clear areas. Thus, large data gaps still exist. This also implies that cloud motion vectors possess an inherent bias toward meteorologically active areas which produce clouds so that their statistical averaging for climatological purposes may not be valid. (Hinton, 1977)

    A potential solution to this data deficiency lies in the water vapor data available from geostationary satellites such as the METEOSAT and the VAS. Unlike most gases in the atmosphere, water vapor is not well mixed. Water vapor is also a conservative substance which is advected by the atmospheric winds. Thus the inhomogeneities of the water vapor being advected by the winds can be considered as potential tracers which could be used to remotely obtain wind information.

    Using moisture as a tracer was first attempted by Rossby (1937) using specific humidity plotted on isentropic charts. Rossby observed that tongues of maximum or minimum moisture content advanced less rapidly than one would expect from the observed wind distribution indicating intense mixing between the tongues and their environment.

With the advent of meteorological satellites with water vapor sensors, interest in the use of water vapor as a meteorological tracer tool was revived. Some of the early TIROS satellites had radiometric sensor centered in the water vapor absorption region near 6.3 μm. The data was used to map relative humidity in the upper atmosphere (Raschke and Bandeen, 1967). A greatly improved water vapor sensor, the Temperature Humidity Infrared Radiometer (THIR) was flown on the Nimbus 4, 5, and 6 spacecrafts. This sensor had a 22 km field of view for the 6.7 μm channel and an associated 11.5 μm infrared channel. The portions of the atmosphere which contribute most strongly to the water vapor 6.7 μm emissions lie between 250 mb and 500 mb. The Nimbus THIR data has been used by Allison et al. (1972) and Steranka et al. (1973) to make global analysis of moisture and wind fields. Qualitative comparisons of moisture patterns on the 6.7 μm images and the 400 mb conventionally measured wind fields indicated that the moisture patterns were generally aligned with the wind field. This fact was used to produce streamlines from a qualitative analysis of the 6.7 μm images.

The feasibility of using water vapor images as a tracer to obtain winds was first demonstrated by Mosher (1977) using loops of 12 hour between consecutive overpasses of the Nimbus THIR in the tropical regions. Kästner, et al. (1980) showed similar results using loops of 1 3/4 hours between consecutive orbits in the polar regions.

The launch of the European geostationary satellite Meteosat in 1977 with a 5 km field of view water vapor sensor provided an opportunity for loops of water vapor images every half hour. Johnson (1980) demonstrated with Meteosat data that a spatially uniform global wind set could be produced from tracking water vapor and clouds. Eigenwillig and Fischer (1981) showed the feasibility of tracking small scale details of pure water vapor structures in

Meteosat images. Their computations placed the water vapor vectors between 400 and 500 mb. Comparisons with radiosonde winds gave RMS differences of 4.9 m/sec for wind velocity. Endlick and Wolf (1981) applied automatic cloud tracking techniques to water vapor images and successfully obtained vectors. They did not attempt to distinguish between cloud structure and pure water vapor structure in their study.

II. Cloud Tracking Background

Tracking water vapor structures to obtain winds is an extension of the technology developed to obtain winds from cloud motions on geostationary satellite images. In order to obtain winds from satellite images one needs:

- a series of satellite images with good geometric fidelity
- a system to receive and store the data
- information on the earth location of the data being processed
- a system to process the data
- a method of identifying a conservative tracer
- a method for tracking this tracer
- a method for determining the height of the tracer
- quality control of the resultant products.

The spin-scan radiometers on the Meteosat and GOES-VAS satellites provide images of visible, 11 micron infrared, and 6.7 micron water vapor data. The spinning satellite produces a series of images which have the geometric fidelity to obtain aligned images loops. In this study we used Meteosat and VAS digital data on computer tapes obtained from the Meteosat and VAS digital mass store archives. The McIDAS (Chatters and Suomi, 1975) at the University of Wisconsin was used to process the data in a man-interactive mode, with a person selecting the tracers to be tracked.

To be a valid tracer of the wind a feature must be a quasi-passive shallow

body drifting with the wind during the time of the series of images being used. Clouds have been shown to be suitable tracers even though there is some evolution during the tracking period. Water vapor inhomogeneities also appear to be valid tracers. The "trackability" of the water vapor inhomogeneities depends upon the ability to distinguish a feature which is small enough to represent a uniform flow of air and yet large enough to have a lifetime long enough to allow the feature to be identified over the interval of several images. The dispersion by atmospheric turbulence of water vapor tracers in the atmosphere depends upon the size of the tracer and the effective eddy diffusivity of the atmosphere. Bauer (1974) in a review of experimental data on the horizontal spreading of inert tracers shows that a tracer with 100 km width will have a lifetime of one day. (Depending on the eddy diffusivity the 100 km feature can have life times from 3 hours to 3.4 days.) A 10 km feature will have a life time of approximately 1 hour.

Figure 1a shows a water vapor image from the Meteosat satellite for August 23, 1978 at 12:00 GMT. The very bright spots are high clouds. The fuzzy white features are water vapor inhomogeneities. The dark features are dry regions. Figures 1b shows the corresponding infrared image and 1c shows the visible image.

The brightness of the water vapor features depends upon the amount of water vapor, and its height. If a given water vapor structure becomes higher, it gets brighter. If this same structure gets more water vapor, it also becomes brighter. Hence it is not possible to determine the tracer height exactly if the mixing ratio is not known, which it generally isn't. Using climatological atmospheric and moisture profiles, Allison et al. (1972) showed that the peak contribution to the water vapor image signal came from the region around 400 mb. Johnson (1980) and Eigennillig and Fischer (1981) showed that on the average, winds obtained from water vapor images correlated
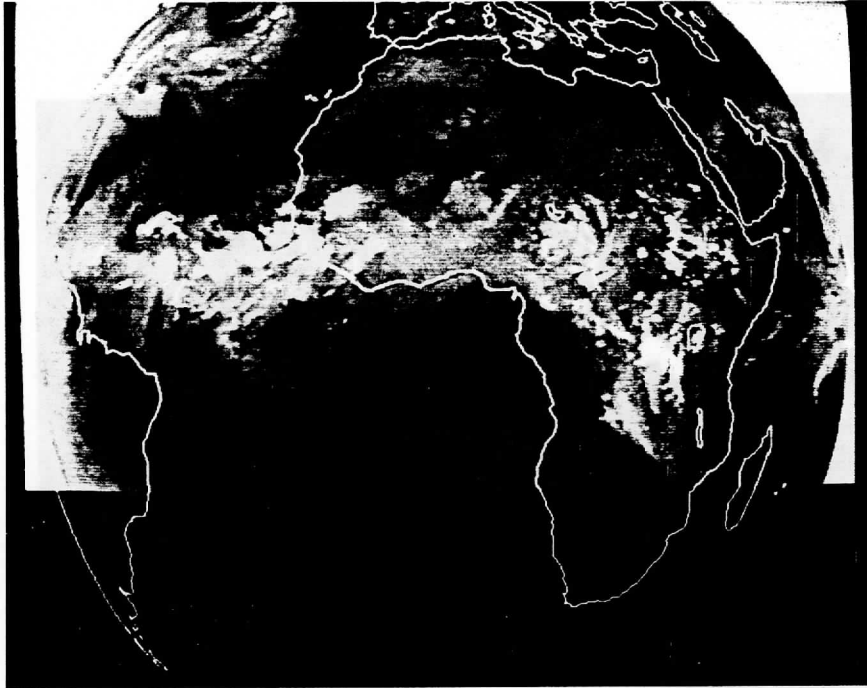
Figure 1a. Water vapor image from the Meteosat satellite for August 23, 1978 at 12:00 GMT. The bright features are high clouds. The gray fuzzy features are water vapor. The dark features are dry regions.
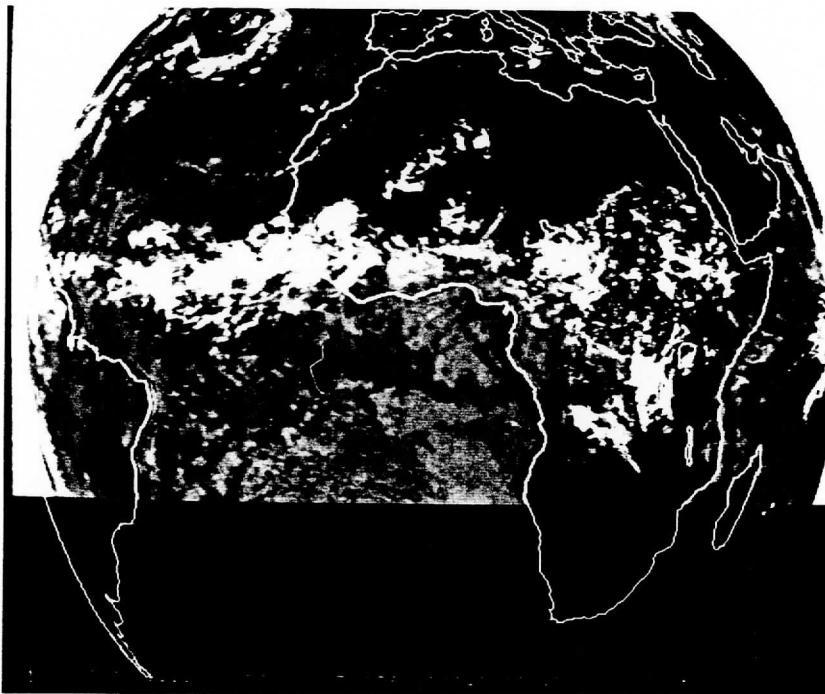

Figure 1b. The infrared image which corresponds with Figure 1a.
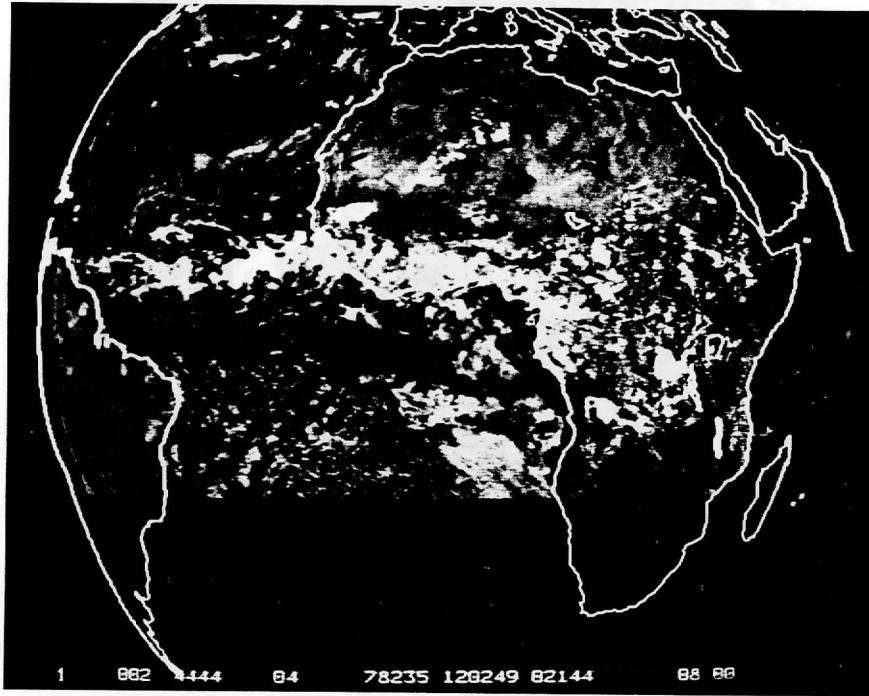
Figure 1c. Visible image which corresponds with Figure 1a.

best with radiosonde winds in the 400 mb region.

However, on a case by case basis, the contribution function for water vapor can vary substantially because of varying amounts of water vapor in the atmsophere, varying heights of the water vapor, and varying temperature profiles. A contribution or weighting function shows the amount of the satellite image signal which comes from different altitudes. Figure 2a shows the water vapor contribution function calculated from observed radio-sonde temperature and humidity profiles of May 8, 1981 near Rapid City S.D. which is at the center of a cyclone. The peak is at approximately 400 mb. Figure 2b shows the contribution function calculated for Little Rock which was in the warm sector of the storm. The peak of the function is approximately 300 mb, and the function is much sharper than figure 2a. Figure 2c shows the contribution function for Bismark which was near the jet core region. Because of the varying altitudes of the moisture in the atmosphere, the contribution function is quite broad and has a double peak, one at 400 mb and another at 600 mb. Hence it is not possible by looking at the water vapor image alone to determine the height of the tracer. The tracer will be somewhere in the middle atmosphere between 300 and 700 mb, but the exact height cannot be determined from the sensed infrared signal and must be inferred from other information.

III. Data Processing

The purpose of this study was to determine the validity and particular characteristics of water vapor tracked winds. In particular we looked into what preprocessing, such as filtering or enhancements, was required of the water vapor images, what was the optimal time interval between water vapor images, could the water vapor features to tracked with correlation type tracking, how could the heights be assigned, and how the water vapor winds
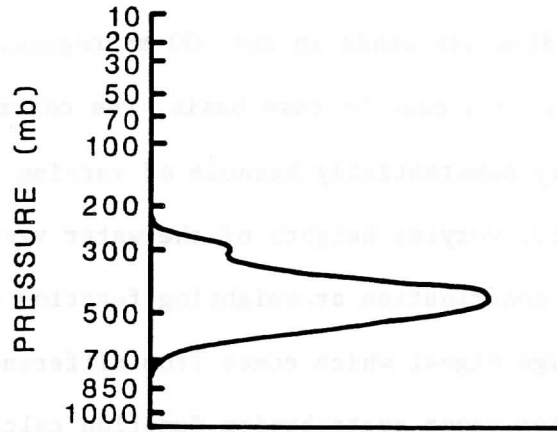
Figure 2a. Water vapor weighting function calculated from the observed radiosonde temperature and humidity profile on May 8, 1981 near Rapid City, S.D., which is at the center of a cyclone.
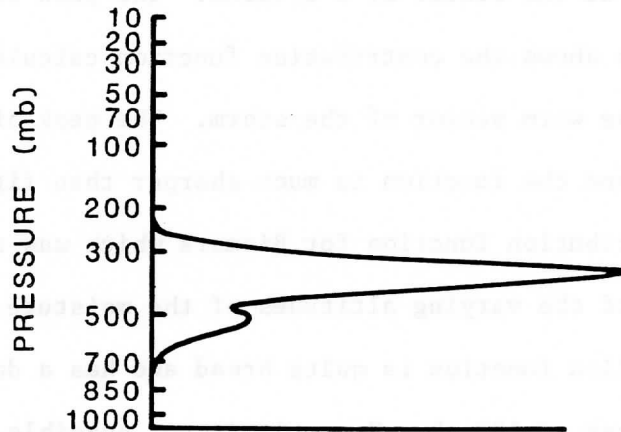
Figure 2b. Water vapor weighting function calculated for Little Rock, which is in the warm sector of the storm. The peak is sharper and higher than the peak of Figure 2a.
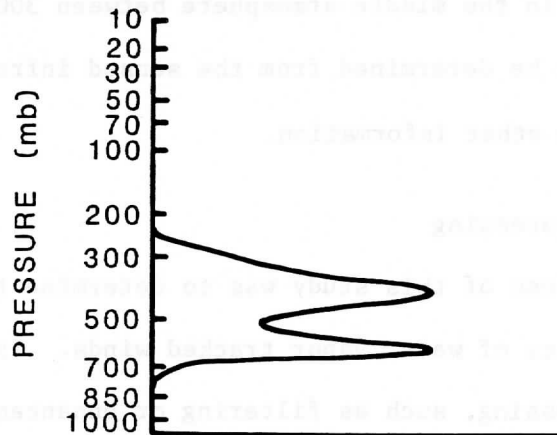
Figure 2c. Water vapor weighting function for Bismark, N. D. which is near the jet core region. The variation between different weighting functions illustrates why it is not possible to determine the height of the water vapor tracers using only water vapor image data.

related to cloud tracked winds and radiosonde winds.

The image data we used for this study came from the Meteosat satellite, and the GOES-4 VAS multispectral image data. The Meteosat has three channels, visible, thermal (11 micron), infrared and water vapor (6.7 micron) infrared, with an infrared spot size of 5 km (Morel, 1978). Images are operationally produced over 30 minutes by the European Space Agency (ESA). The GOES VAS has 12 infrared spectral bands (Smith, et al., 1981) with a filter wheel used to select the desired channel. While there are three water vapor channels on VAS, only channel 8, the 6.7 micron channel was used for this study. The VAS data was taken in the multipectral image (MSI) mode with one scan per image step. The infrared sensors used had a spot size of 14 km. The GOES-4 used in this study had one of the infrared sensors which failed leaving every other scan line blank. The data was preprocessed by filling in the blank lines with the average of the spots on either side of the blanks. The VAS was still an experimental satellite, and the scheduling was controlled by VAS team scientists. The data used in this study had one hour between water vapor images.

Most of the processing done on this study used VAS data. We originally tried to use Meteosat data exclusively. We were supplied a set of 3 Meteosat raw images with half an hour between images from August 23, 1978 at 12:00 GMT. No orbit and attitude information was supplied by ESA. We forced a navigation and computed the offset between the visible, infrared, and visible data using high clouds which were distinct on all three data channels. After obtaining aligned loops of data we produced cloud tracked winds. Satisfactory data sets were obtained from the visible and infrared, but the water vapor tracked data set was not entirely satisfactory. The

water vapor features were quite fuzzy without sharp edges, and the displacement in half an hour was not sufficient to determine an accurate starting and stopping point for the vector computation. We then ordered another data set from ESA which had longer time intervals between images. ESA sent data which had been "processed" from their archive. We were able to obtain orbit and attitude information from ESA, but not betas which give the east-west shift of the data. Without the betas we were not able to obtain a satisfactory navigation and image alignment.

Rather than spend more effort on trying to use the Meteosat data, we used VAS data for the rest of the study. VAS has the same spectral channel for water vapor images as the Meteosat, but has a coarser spatial resolution of 14 km vs. 5 km of the Meteosat. The missing infrared detector of the VAS which caused every other line to be blank further reduced the resolution in the north-south direction. However, since the water vapor features have a fuzzy appearance and are generally quite large, the course resolutuion of VAS was not a major detriment to this study.

A. Preprocessing Water Vapor Data

We investigated the need to preprocess the water vapor data to help bring out features which can be tracked. Figure 3a shows a VAS water vapor image of the full disk. There is not a large range of gray scales in the image. We tried enhancing the image through gray scale stretching, false coloring and using digital filters. Eigenwillig and Fischer (1981) used high pass filters successfully, while Mosher (1977) used equal population gray scale stretching. Johnson (1980) used sliced gray scale stretching.

The digital filters used were one dimensional high and low pass filters. The high pass filter applied to the Meteosat data tended to bring out the
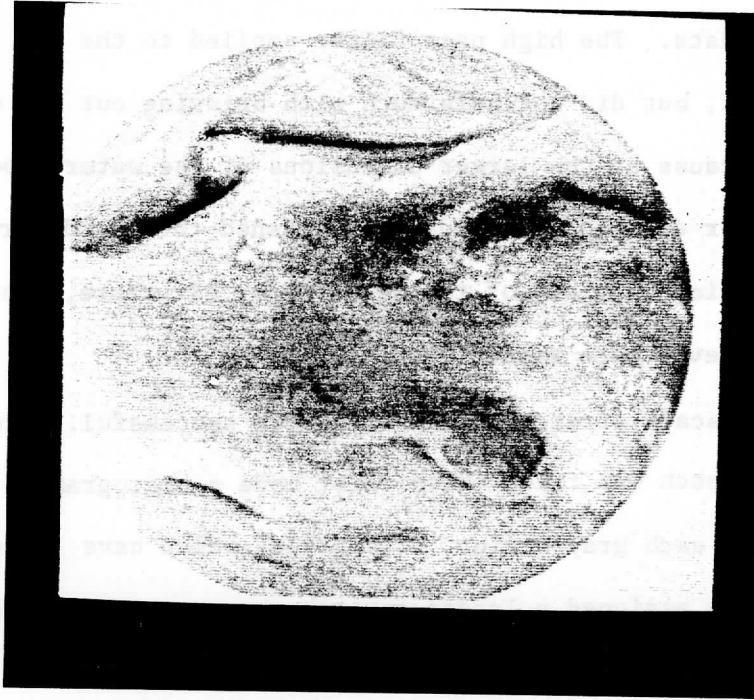
Figure 3a. GOES-4 (VAS) water vapor image from December 11, 1980 at 15:00 GMT with no enhancement.
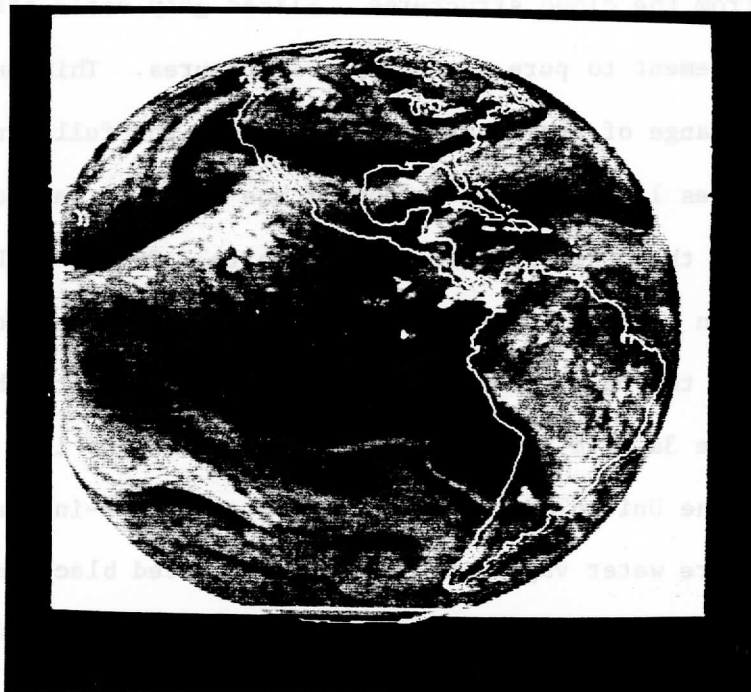

Figure 3b. VAS water vapor image of Figure 3a with a sliced gray scale stretch enhancement applied to the image to bring out the pure water vapor structure.

noise in the data. The high pass filter applied to the VAS data brought out the clouds, but did not help much with bringing out the water vapor structures because of the larger dimensions of the water vapor structure. A low pass filter applied to the data diminished the cloud structure somewhat, but did not bring out any of the water vapor structure, just causing the image to look even more washed out.

The gray scale stretching was much more successful. A equal population gray scale stretch was tried which first made a histogram of the number of occurrences of each gray scale. Gray scales which have large number of occurrences are assigned a larger stretch than gray scales which have fewer occurrences. This gave an esthetically pleasing image which showed the water vapor structure in addition to showing the cloud structure. This would be the recommended preprocessing to be done if both high clouds and water vapor were to be tracked on the same image.

In this study we wanted to track the pure water vapor structures separately from the cloud structures. Sliced gray scale stretching gave greater enhancement to pure water vapor structures. This enhancement has a narrow range of gray scales expanded into the full range of gray scales. Any input values less than the bottom of the slice is set to black and input values greater than the slice are set to white. On the McIDAS this slice enhancement can be done interactively using the joy stick to control the enhancement of the television image being viewed. Figure 3b shows the VAS image of figure 3a with a slice enhancement applied to it. Figure 3c shows a blow up of the United States sector of 3b. For man-interactive cloud tracking of pure water vapor structures, the sliced black and white enhancement was judged most useful in bringing out features to track. We also tried

Figure 3c. Blow up of the United States sector of Figure 3b.

putting in false colors rather than black and white enhancement, but this
was judged as detrimental in that it generally made the features harder to
see and did not bring out new features.

B. Water Vapor Wind Height Assignment

As discussed in section II, the water vapor features being tracked
are in the middle troposphere, but the exact level is not possible to
determine from the satellite data alone. The brightness of the image feature
is determined both by the water vapor concentration and the temperature
(height) of the water vapor. Hence, the sensed radiation cannot be used to
compute the height as the infrared window channel can be used to get cloud
heights. While previous studies (Eigenwillig and Fischer, 1981, Johnson, 1980,
Mosher, 1977) have used a climatological height derived from a water vapor
weighting function of standard atmosphere, it has been demonstrated in
section II that the weighting function changes for different synoptic
conditions.

Since the water vapor height cannot be measured directly, we have attempted
to infer the heights indirectly from cloud heights, and then manually
assign the heights to the water vapor features. In some regions, there were
clouds embedded in the water vapor features so the heights were easy to
obtain. (However since there were clouds within the water vapor, the cloud
motions could give winds which limits the value of the water vapor winds).
In many areas of interest, particularily around the jet, there are not clouds
embedded in the water vapor structures, or even in the vicinity. Figure 4a
shows the VAS water vapor image over the southeastern United States on
December 11, 1980 at 15Z. The dark dry feature is caused by the descending
jet stream. Figure 4b shows the infrared image for the same area. While
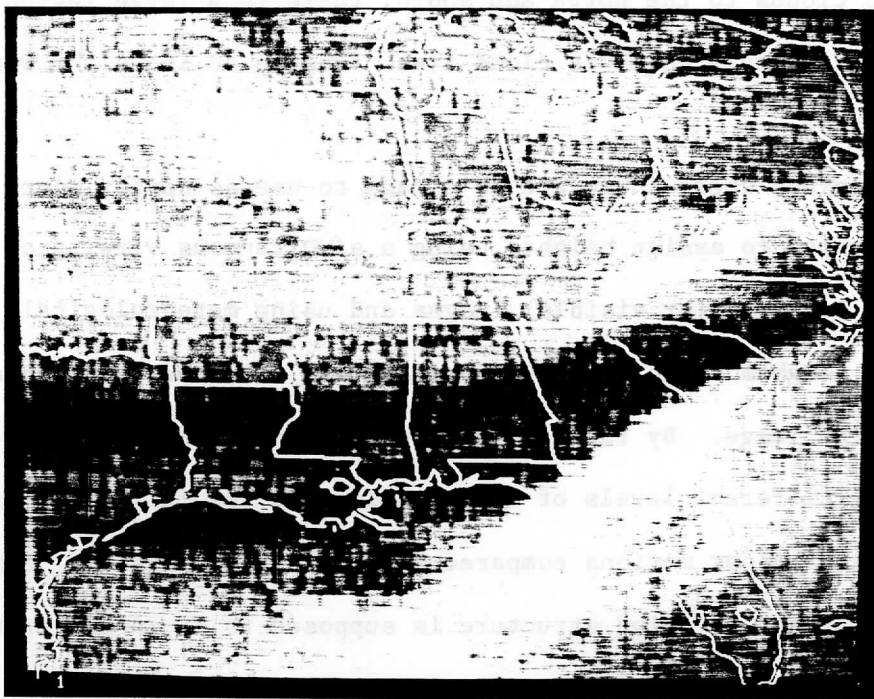
Figure 4a. VAS water vapor image on December 11, 1980 at
15 GMT over the southeastern United States. The dark, dry
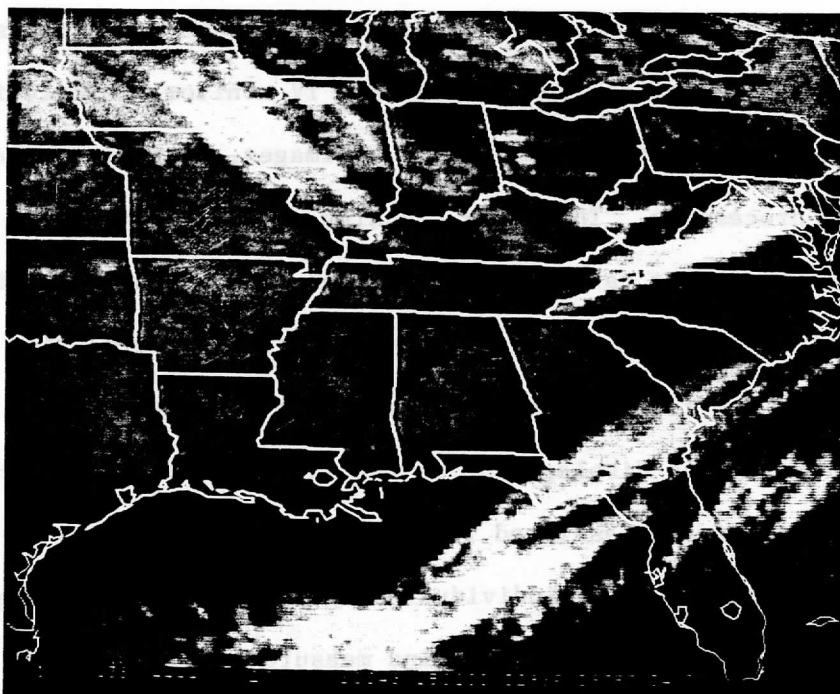feature is caused by a decending jet.

Figure 4b. VAS 11 micron infrared image which corresponds to
Figure 4a. There are no clouds in the vacinity of the jet which
shows up on Figure 4a.

there are clouds to the north and south, there is a large region around the
water vapor feature which is cloud free. Figure 4c shows the visible image
for this area.

In regions where there are no clouds to use as height bench marks, we
have attempted to assign heights using a simultaneous viewing of both water
vapor and infrared (or visible) images and using meteorological judgement
to assign heights. The water vapor image was enhanced and then added to
the infrared image. By rapid looping of the combined images, it was possible
to see the different levels of cloud motions on the infrared images and to see
how the water vapor motions compared with the cloud motions. Using meteorological
judgement of how the wind structure is supposed to be in different parts
and heights of synoptic situations, the water vapor motions were subjectively
assigned heights using the cloud heights as benchmarks.

C. Water Vapor Tracking

The water vapor tracking was done on the Man-computer Interactive
Data Access System (McIDAS) at the University of Wisconsin-Madison. The
McIDAS allows loops of aligned images on a TV monitor, interactive enhancements
of the images, interactive combination of images, graphic overlays, and
interactive processing. The cloud tracking procedures (Mosher, 1979) allow
for a person to do the target identification, and to supply a first guess target
displacement by having a cursor follow the target. Correlation algorithms
then fine tune the first guess displacement, or a manual option is available
where the first guess displacement is the final displacement. Heights can
either be automatically assigned from cloud top temperatures or can be
manually assigned to either individual targets or fleets of targets. Loops
of three images were used with the wind measurements being made with each
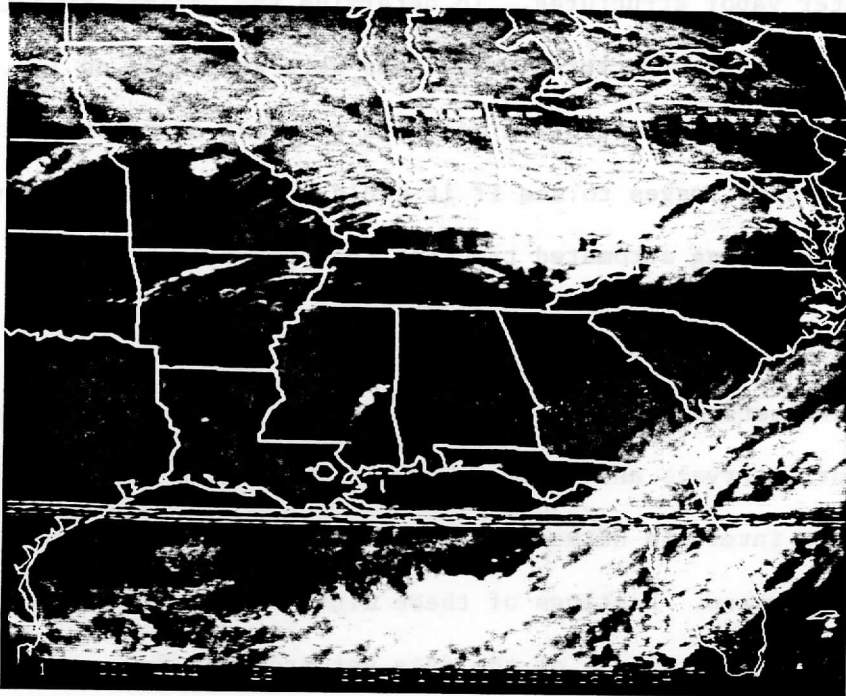pair of images.

-17-

Figure 4c. Visible image which corresponds to Figure 4a.

Wind data sets were generated using visible clouds, infrared clouds, and pure water vapor structures. To determine the optimal time interval for tracking water vapor structures, wind sets were generated on 1/2, 1, 2, and 3 hour intervals. Also attention was paid to using correlation tracking on the water vapor images to see if it would be possible to make water vapor wind sets using automated tracking techniques.

D. Analysis of Results

Wind sets were generated on August 23, 1978 using Meteosat data with 1/2 hour intervals and on December 11, 1980 using VAS data with one, two and three hour intervals between images. Visible, infrared and water vapor winds were generated. Listings of these winds are contained in the appendix. The following is an analysis of the data set produced from the VAS water vapor images. Wind data was produced for the full disk, but radiosonde data was only available over the United States, hence most of the analysis will be centered on the United States region. Figure 5a shows the 300 mb radiosonde winds over North America. Figure 5b shows the 400 mb and figure 5c shows the 900 mb radiosonde winds for December 11, 1980 at 12GMT. Figures 6a and b show the visible and infrared images which cover North America. Figures 3 and 4 are also from this time period. There is a cutoff low off the southern California coast, a ridge over the Rocky Mountains, a large trough the axis extending from east of Hudson Bay to Louisiana, and a frontal system off the east coast of North America. The radiosonde data shows a polar jet core coming down over the Dakotas and a jet core exiting New Jersey coast. There is a subtropical jet coming across Texas.

Cloud tracked winds were produced as were water vapor winds for this time period. Three water vapor wind sets were made with 1, 2 and 3 hour
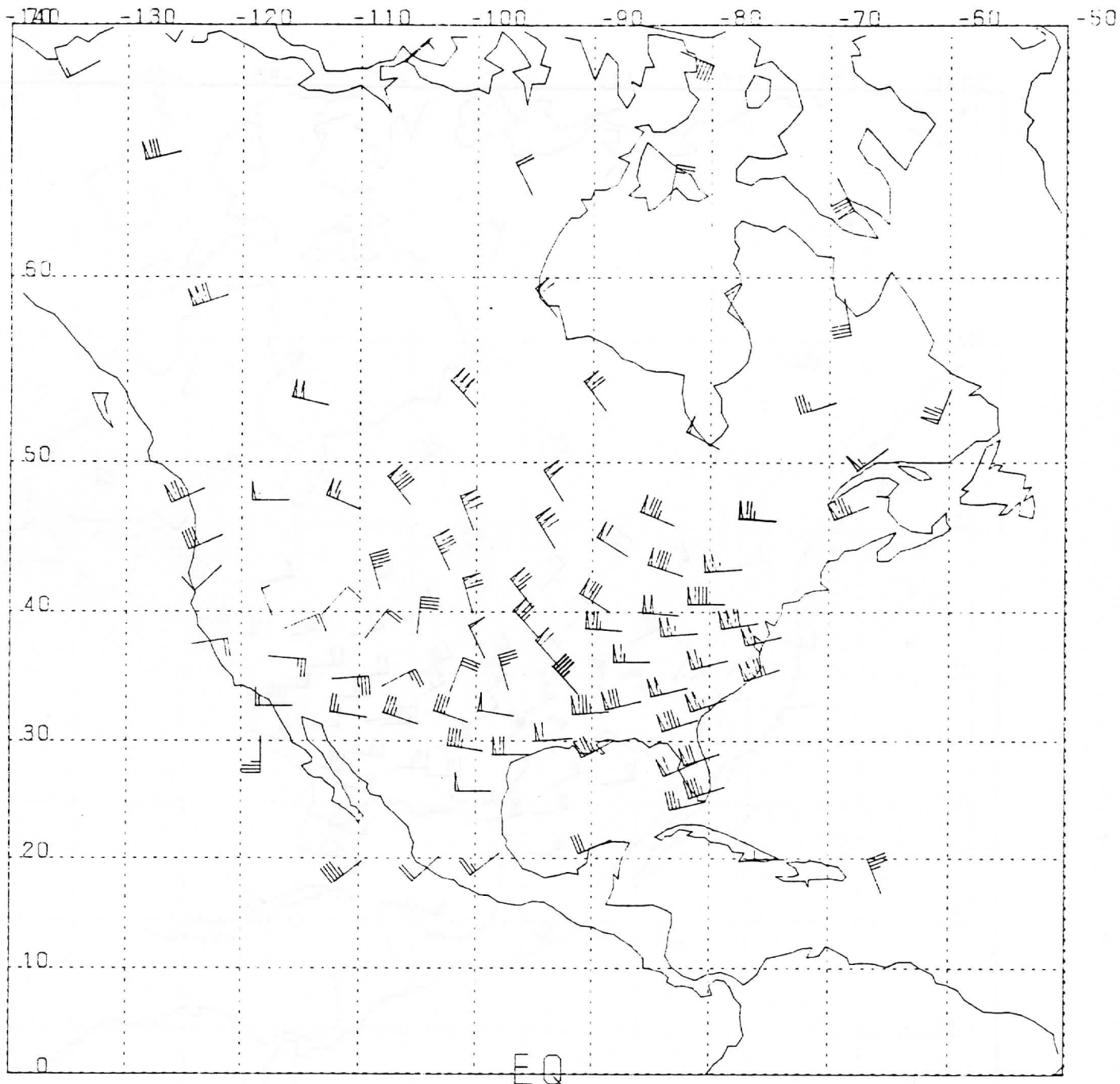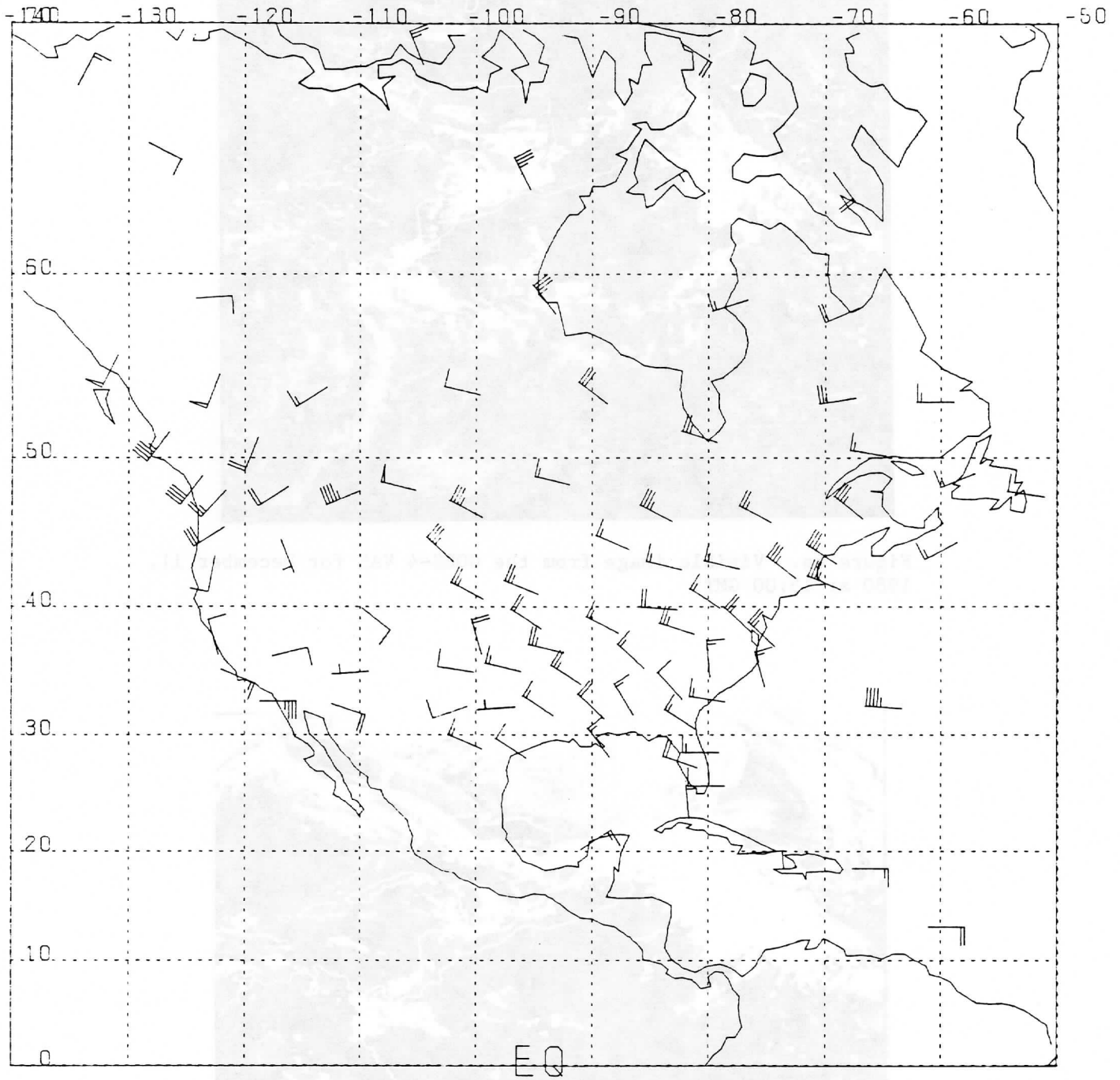
DAY2680346 TIME120000   350- 100 MB

Figure 5a.   The 300 mb radiosonde winds over North America for
December 11, 1980 at 12:00 GMT.
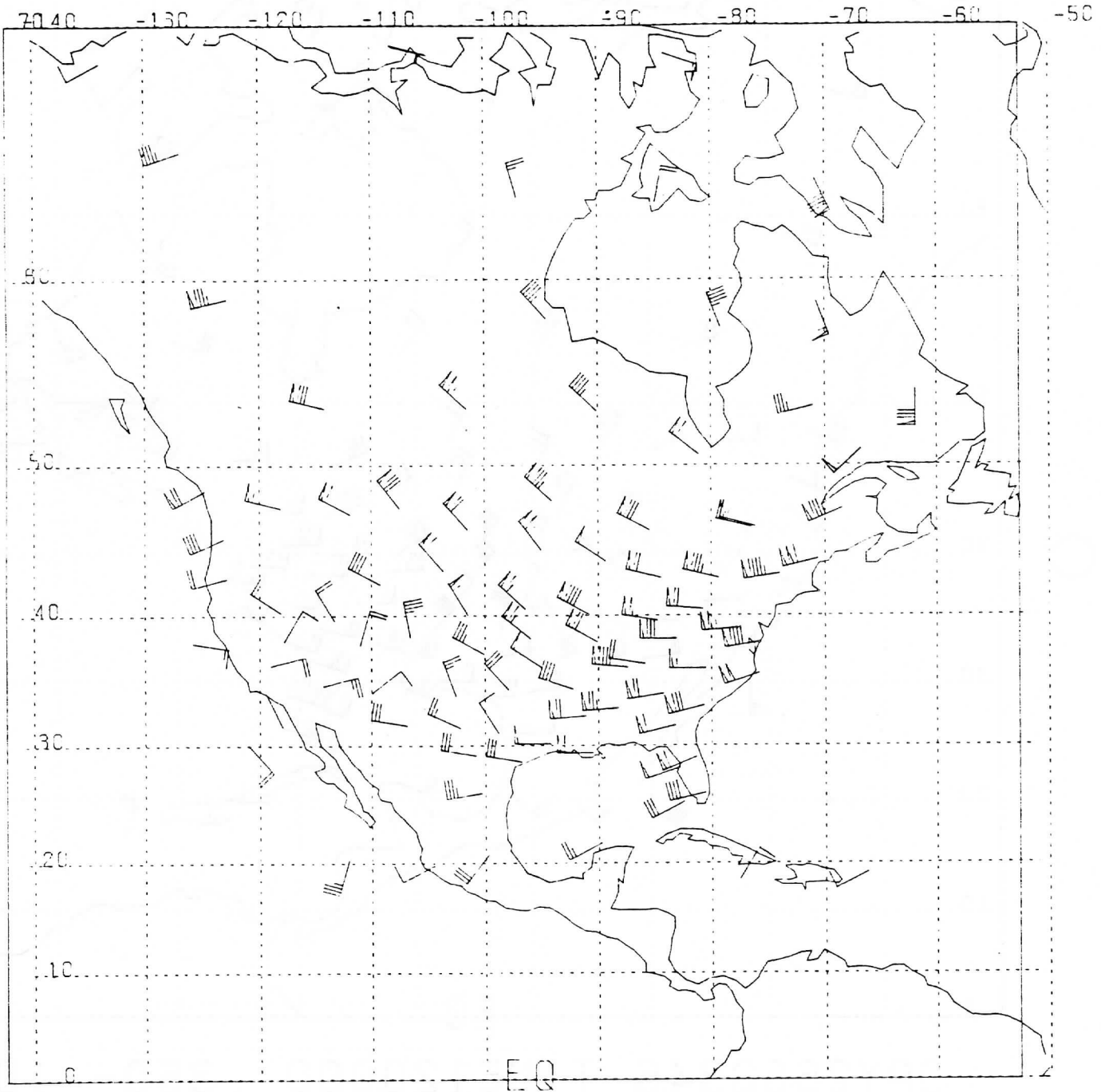
DAY2680346 TIME120000 450- 350 ME

Figure 5b. The 400 mb radiosonde winds over North American for
December 11, 1980 at 12:00 GMT.

DAY2680346 TIME120000 999- 651 MB

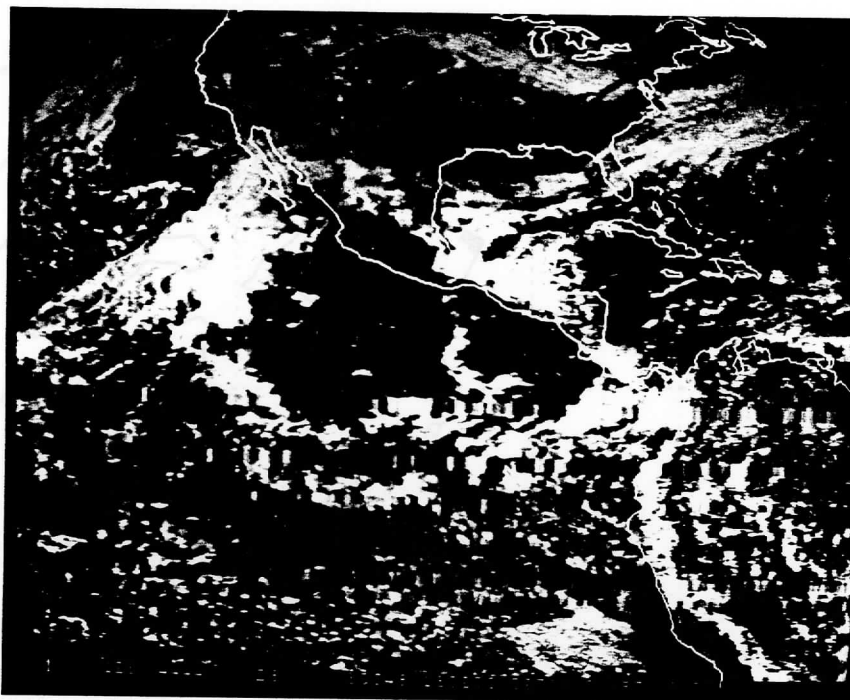Figure 5c. The 900 mb radiosonde winds over North America
at 12:00 GMT.

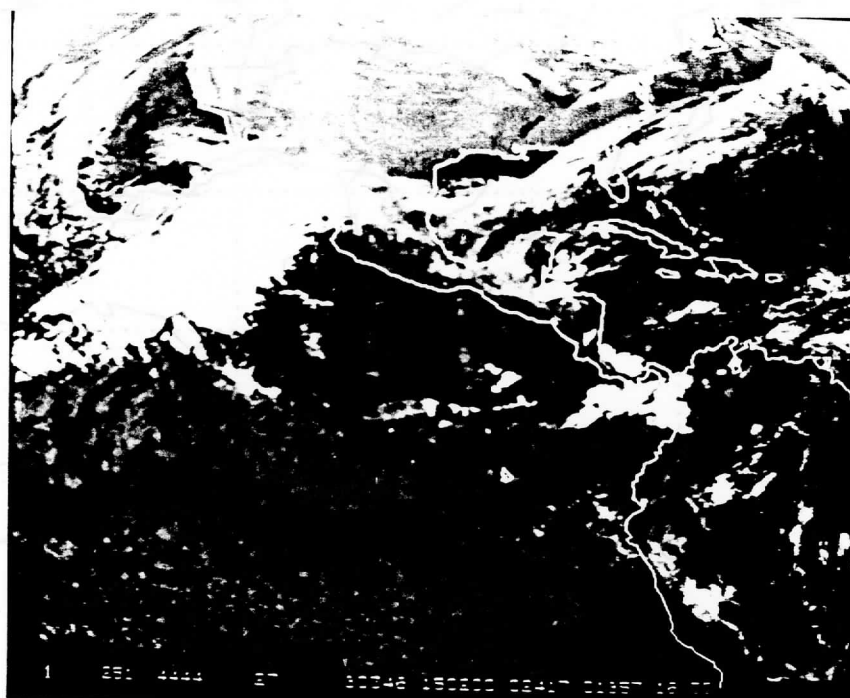Figure 6a. Visible image from the GOES-4 VAS for December 11, 1980 at 15:00 GMT.

Figure 6b. Infrared image which corresponds to Figure 6a.

intervals. Figure 7a shows full disk plot of the water vapor winds with one hour interval which were assigned heights between 500 and 300 mb. There were 131 water vapor winds in this data set. Figure 7b shows the same thing for the two hour winds. There were 120 water vapor winds in this data set. Figure 7c shows the same thing for the three hour intervals there were 86 water vapor winds in this data set. Figure 8a shows the high-level cloud tracked winds for this time period made from the visible and infrared images with one hour intervals. Figure 8b shows the mid-level cloud tracked winds and figure 8c shows the low-level cloud winds.

Water vapor winds determination was possible on all time intervals tried. The one hour interval data set had the most vectors (131), though the two hour set had almost as many (120). The manual tracking of the water vapor features was easiest with the two hour interval data set. The three hour interval data set had a smaller number of vectors (86). The tracking was done over a six hour total interval (3 images in loop with three hours between images) and some of the smaller water vapor features which could be tracked on shorter interval data sets could not be tracked over the full six hours. The cloud tracking was most successful with the shorter time interval.

While correlation tracking was tried on the water vapor features, it was generally not very successful. Only about 10% of the water vapor winds measured were made using correlation. The rest used the "single pixel" method of tracking where the operator manually tracks the feature. The features which were successfully tracked using correlation were the very pronounced features with well defined structure. Most of the targets were too fuzzy for successful correlation tracking.
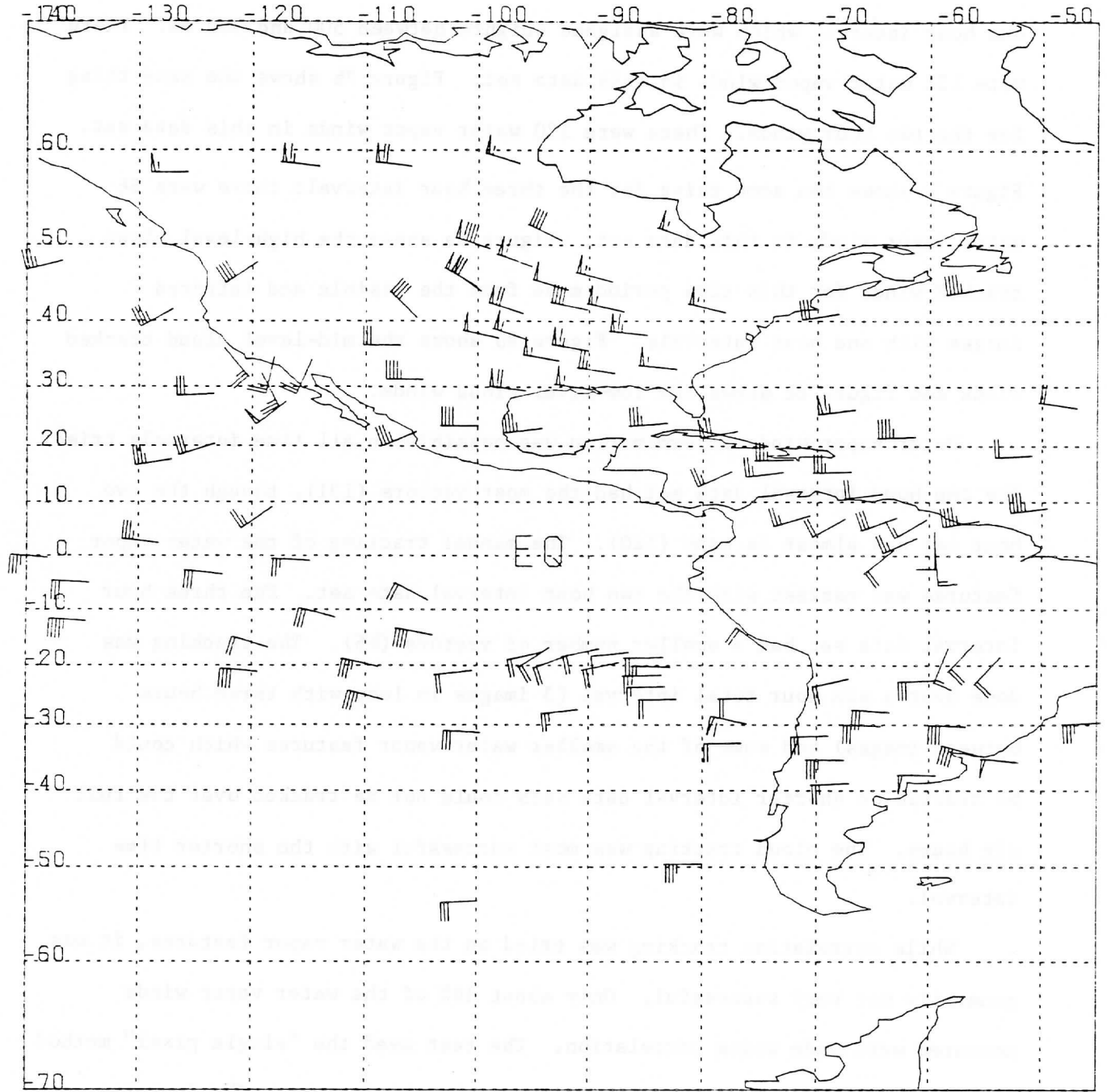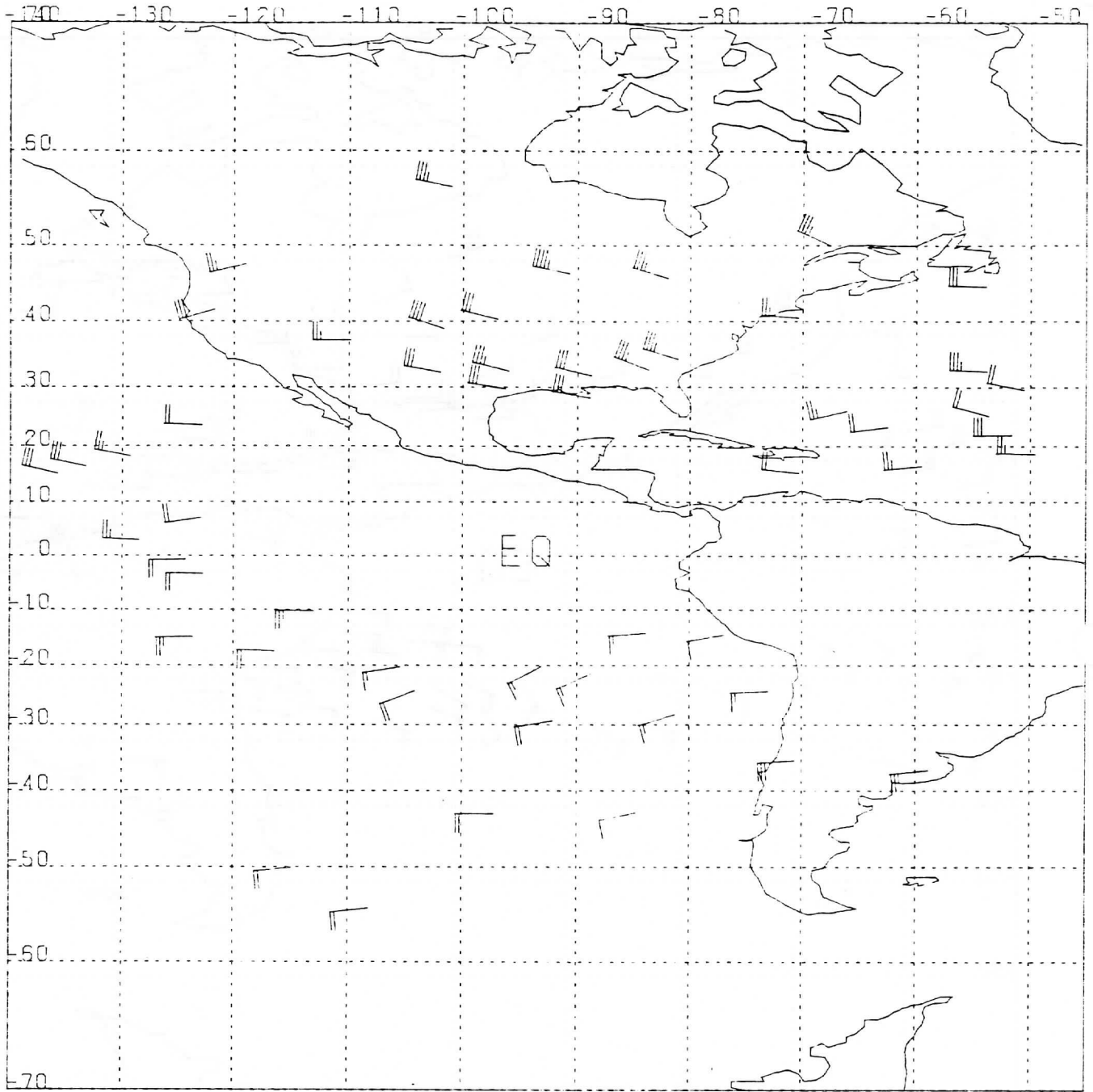
DAY2780346 TIME170200 500- 300 ME

Figure 7 a. Water vapor tracked winds from December 11, 1980 at
17:00 GMT with one hour time interval between images with a total
tracking interval of two hours.
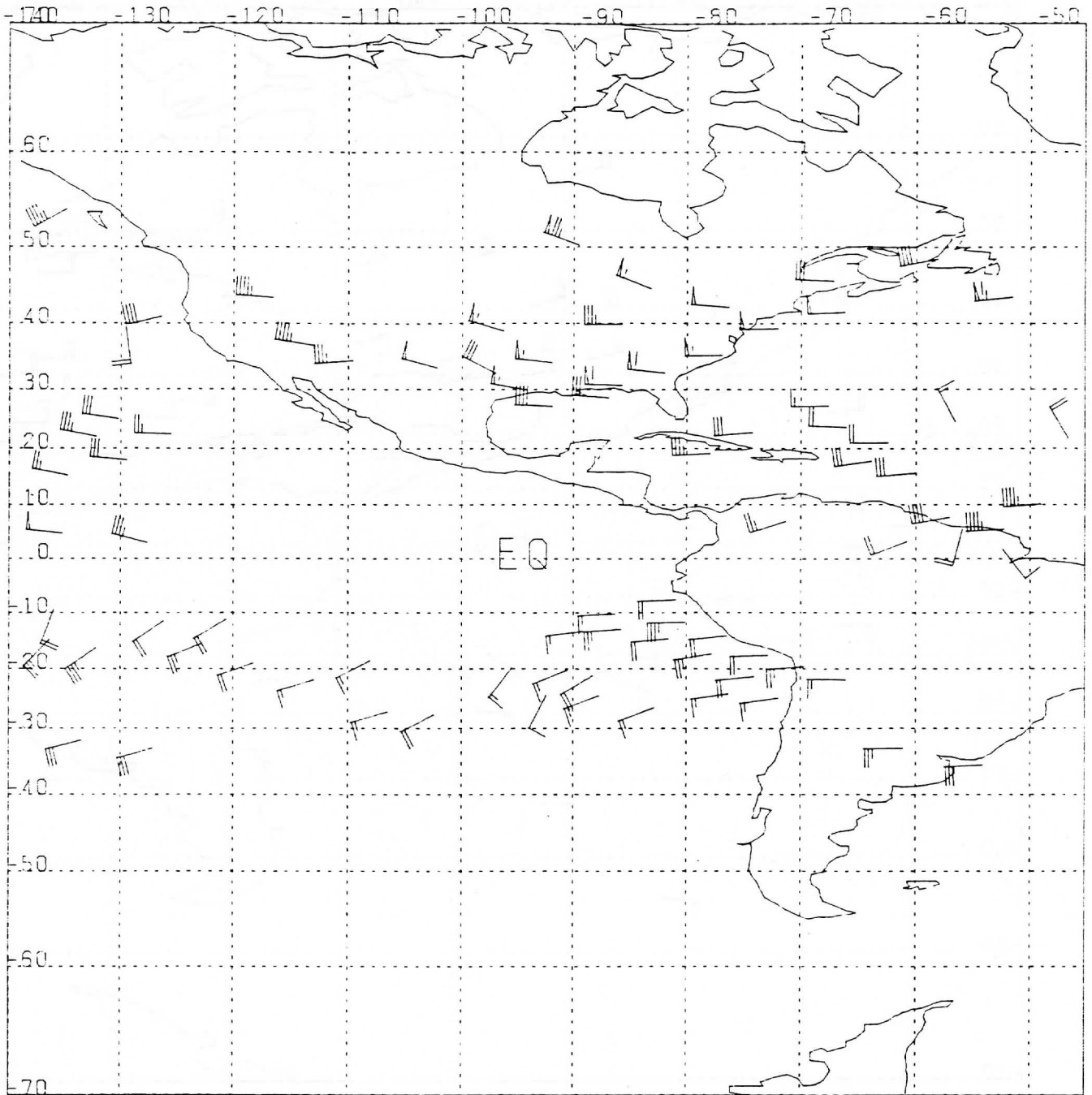
DAY2780346 TIME170200   500- 300 M5

Figure 7b. Water vapor tracked winds from December 11, 1980 with
two hours between images with a total tracking interval of four
hours.

DAY2780346 TIME150200 500- 300 MI

Figure 7c. Water vapor tracked winds from December 11, 1980 with three hours between images with a total tracking interval of six hours.
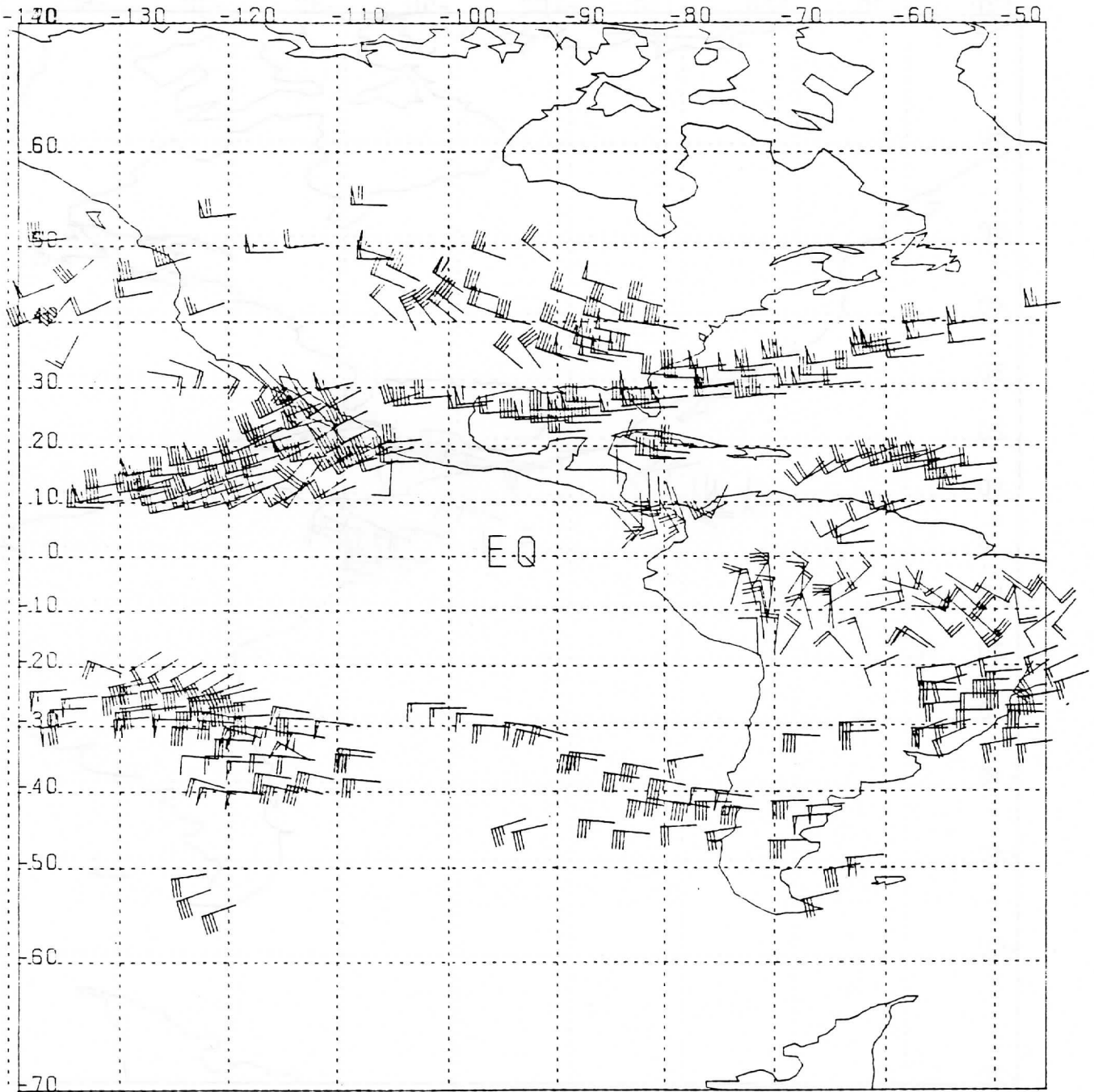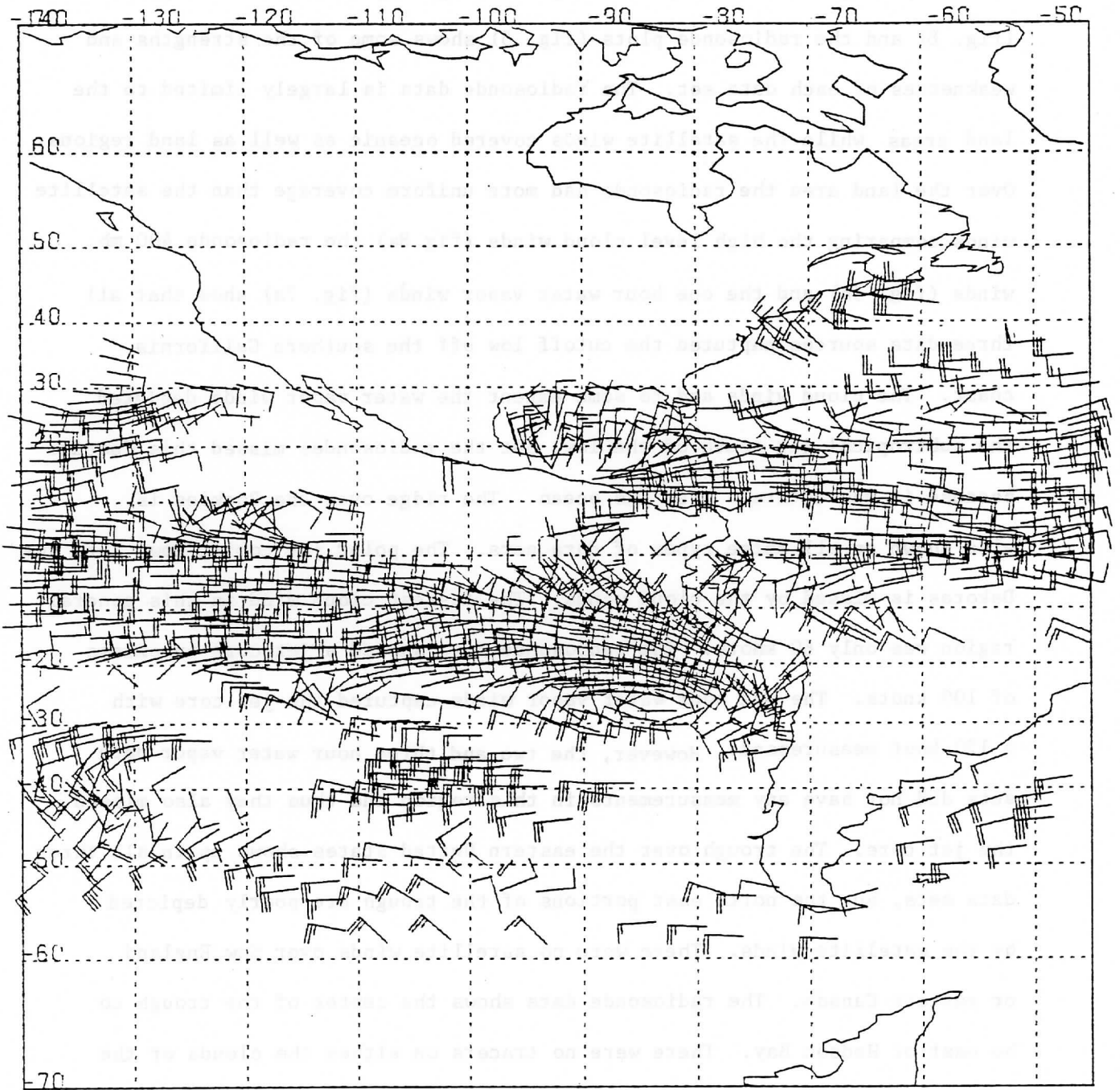
DAY2780346 TIME170200 350- 100 MB

Figure 8a. High-level cloud tracked winds for the same period as
the water vapor tracked winds of Figure 7a.
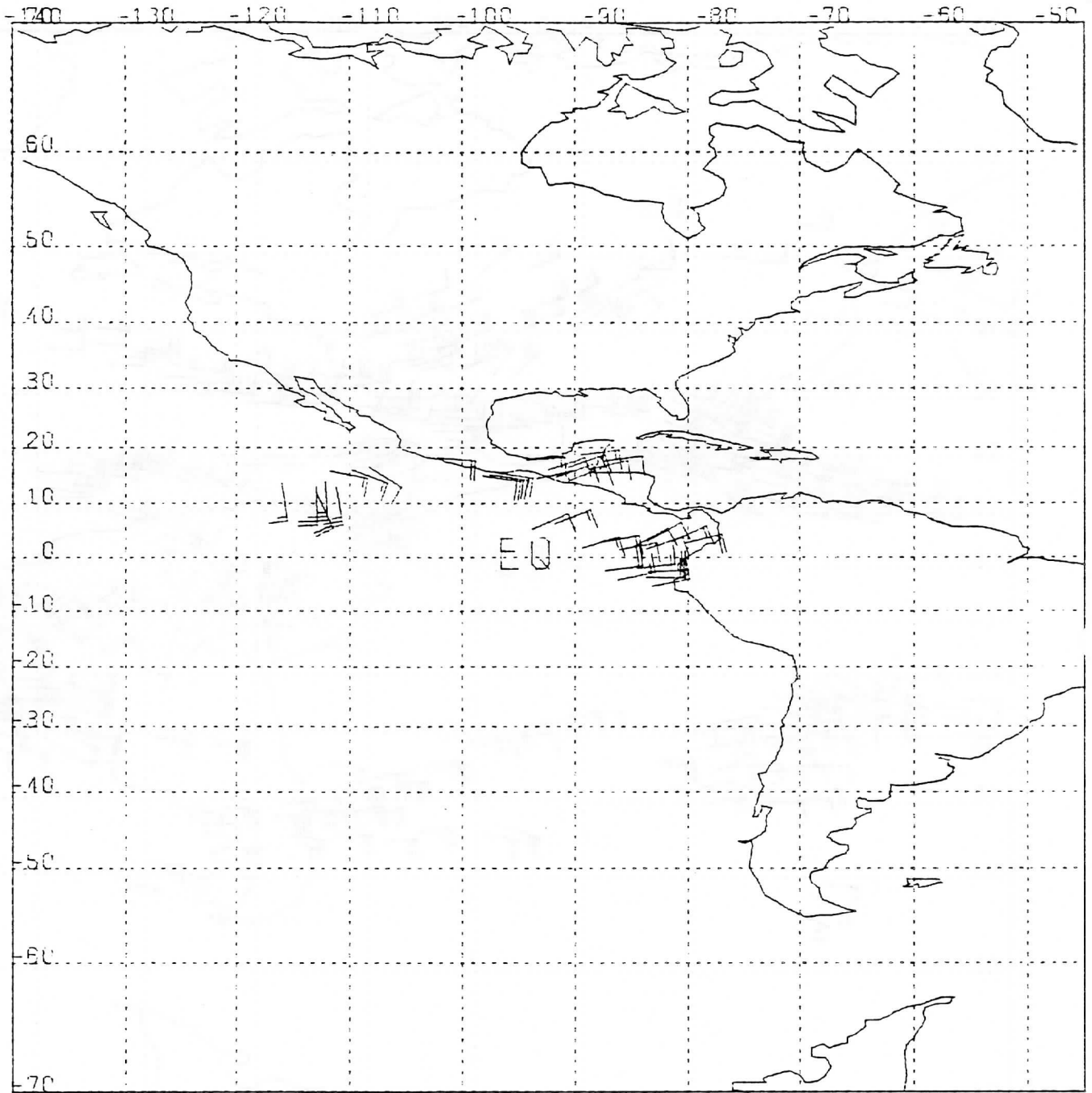
DAY2680346 TIME170200 650- 351 MB

Figure 8b. Mid-level cloud tracked winds for the same time period.

DAY2680346 TIME170200 999- 651 ME

Figure 8c. Low-level cloud tracked winds for the same period.

Comparing the water vapor wind plots (fig. 7), the cloud wind plots (fig. 8) and the radiosonde plots (fig. 5) shows some of the strengths and weaknesses of each data set. The radiosonde data is largely limited to the land areas while the satellite winds covered oceanic as well as land regions. Over the land area the radiosonde had more uniform coverage than the satellite winds comparing the high level cloud winds (fig 8a) the radiosonde 400 mb winds (fig. 5b) and the one hour water vapor winds (fig. 7a) show that all three data sources captured the cutoff low off the southern California coast. The cloud winds and to some extent the water vapor winds depicted the subtropical jet south of the low, but the radiosondes missed this feature because it was entirely over the ocean. The ridge over the Rockies is also shown on all three types of data sets. The polar jet coming down into the Dakotas is missed by the cloud winds. The fastest cloud wind in this general region was only 60 knots. The radiosonde data showed a jet core in excess of 100 knots. The one hour water vapor winds captured the jet core with a 120 knot measurement. However, the two and three hour water vapor data sets did not have any measurements in this region and thus they also missed the jet core. The trough over the eastern United States shows up in all three data sets, but the north east portions of the trough are poorly depicted by the satellite winds. There were no satellite winds over New England or eastern Canada. The radiosonde data shows the center of the trough to be east of Hudson Bay. There were no tracers on either the clouds or the water vapor images in this region so this trough feature was not shown on either satellite data set. The water vapor data set has a 30 knot wind off Long Island while the radiosonde data shows there should be a jet of over 100 knots in this region at this height. The lower lever radiosonde

winds (fig. 5c) show winds closer to this velocity, indicating that the height assignment of this vector is probably too high.

Cloud tracked winds generally are limited to high and low-levels and to regions with cloud available. Consequently there are large regions without satellite wind coverage. In figure 8a there are no high-level winds over the Pacific from 10°N to 20°S, an area of over 22 x 10^6 km^2 without a single high-level wind measurement. Figure 9a shows the composite satellite derived high-level winds. The water vapor winds helped fill in some of the high-level data voids, though not all. The area over the Pacific near the equator still is lacking in winds, as is the New England area. Figure 8b shows the mid-level cloud winds. Except for a small area in the tropics, there were no mid-level clouds available for tracking in this data set. Figure 9b shows the combined mid-level satellite winds. While there still are not as many winds as at higher and lower levels, the addition of water vapor winds significantly increases the mid-level coverage. The low-level cloud winds in figure 8c have very good coverage over the ocean regions. The addition of water vapor winds does not significantly alter the low-level wind coverage. Figure 7c shows the combined satellite low-level winds. The only area which was lacking data in the cloud winds which had low-level water vapor assignments was a small region just north of the equator from 90°W to 110°W, 0°N to 10°N.

The water vapor winds were compared with radiosonde and cloud winds to determine the compatability between the different types of data sets. Data which was within 200 km, 200 mb, and 12 hours was considered nearly co-located and were compared for vector differences. Figure 10 shows cumulative frequency of the vector magnitude differences between the water vapor winds
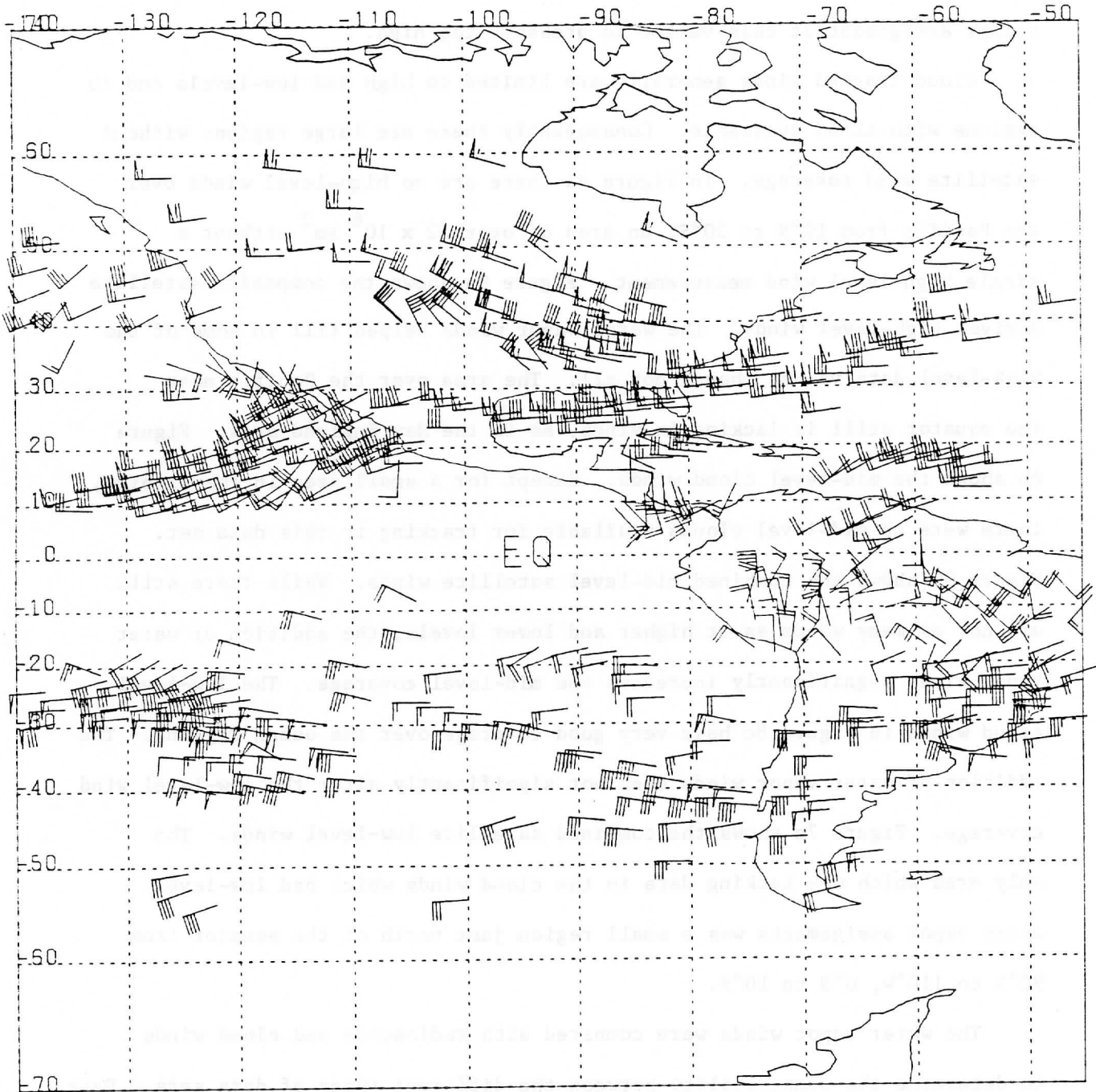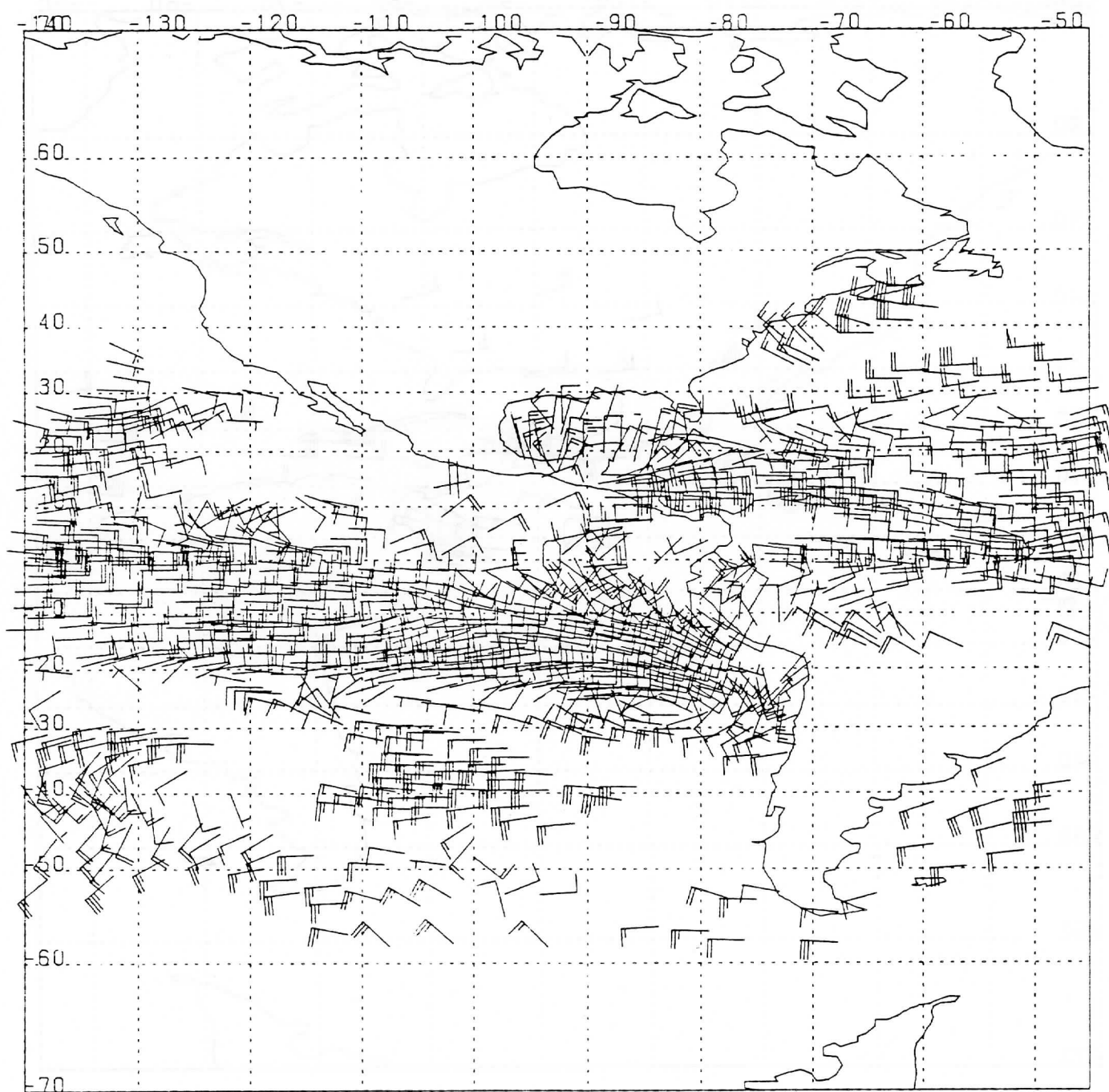
DAY2780346 TIME170200 350- 100 MB

Figure 9a. Combined high-level (350-100 mb) cloud winds and water vapor winds. Compared to Figure 8a (cloud winds only) the water vapor helped fill in some of the data voids over the subtropics, and helped improve the definition of the polar jet coming in over the Dakotas.
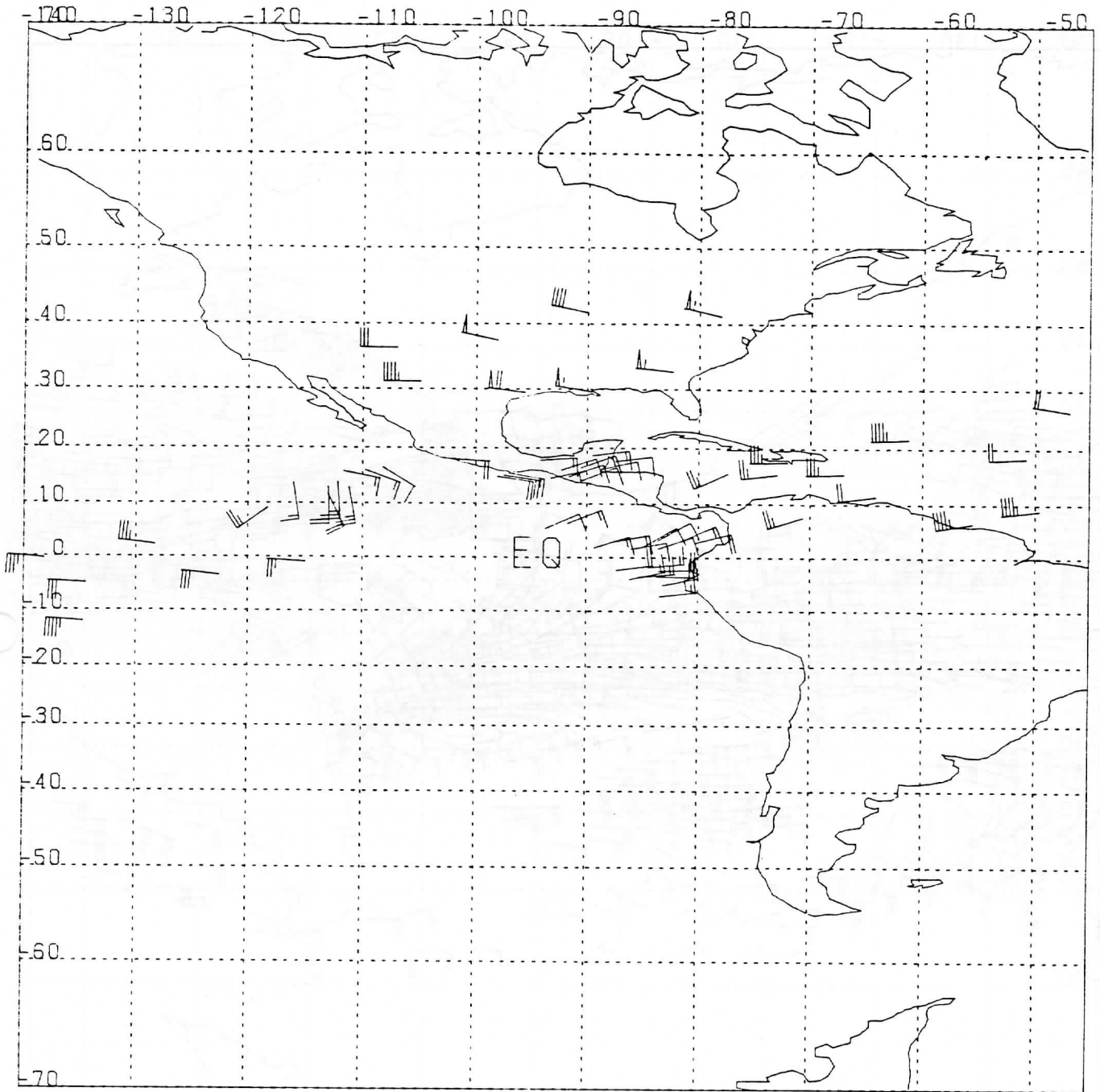
DAY2780346 TIME170200 650- 351 MB

Figure 9b. Combined mid-level (650-350 mb) cloud and water vapor
winds. Figure 8b (cloud wind only) had almost no mid-level vectors.
The addition of water vapor winds significantly increases the mid-
level wind coverage.

DAY2780346 TIME170200   999- 651 MB

Figure 9c. Combined low-level (surface-650 mb) cloud and water
vapor winds. Only a few areas lacking low-level cloud wind coverage
showed any significant increase in coverage with the addition of
water vapor winds.

and the nearly co-located radiosonde winds. The one hour water vapor winds (24 matches) showed a slightly better comparison with the radiosonde data than did the two hour data (56 matches). The mean differences for the one hour data was 15.3 m/sec and 16.7 for the two hour data. The three hour data (41 matches) showed the poorest correlation with radiosonde data. The mean difference was 18.9 m/sec. To illustrate the level of errors to expect from water vapor winds, figure 11 shows FGGE cloud wind comparisons vs. radiosonde data (Mosher, 1980) with the two hour water vapor comparisons shown as the bottom curve on the figure. This shows a slightly lower level of absolute accuracy for the water vapor winds as compared to cloud wind accuracy.

The water vapor winds were compared with nearly co-located cloud winds of this data set. Figure 12 shows a inter-comparison of FGGE cloud winds between different data producers. Superimposed on the graph are comparisons between nearly co-located cloud and water vapor winds, and comparisons between one and two hour water vapor data sets. The comparison between the cloud winds and the one hour water vapor winds (20 matches) shows a slightly worse relationship to other satellite wind data sets than the FGGE cloud winds do. The comparison of one hour water vapor winds to two hour water vapor winds shows a similar relationship to cloud to cloud wind comparisons, showing reasonable consistancy between water vapor data sets.

As mentioned earlier, a 1/2 hour interval Meteosat data set was produced for August 23, 1978 at 12:00 GMT. Figure 1 showed the visible, infrared, and water vapor images used to produce this wind data set. Figure 13 shows the water vapor winds produced from the Meteosat images. Despite the short time interval and the difficulty in tracking features, a considerable number of
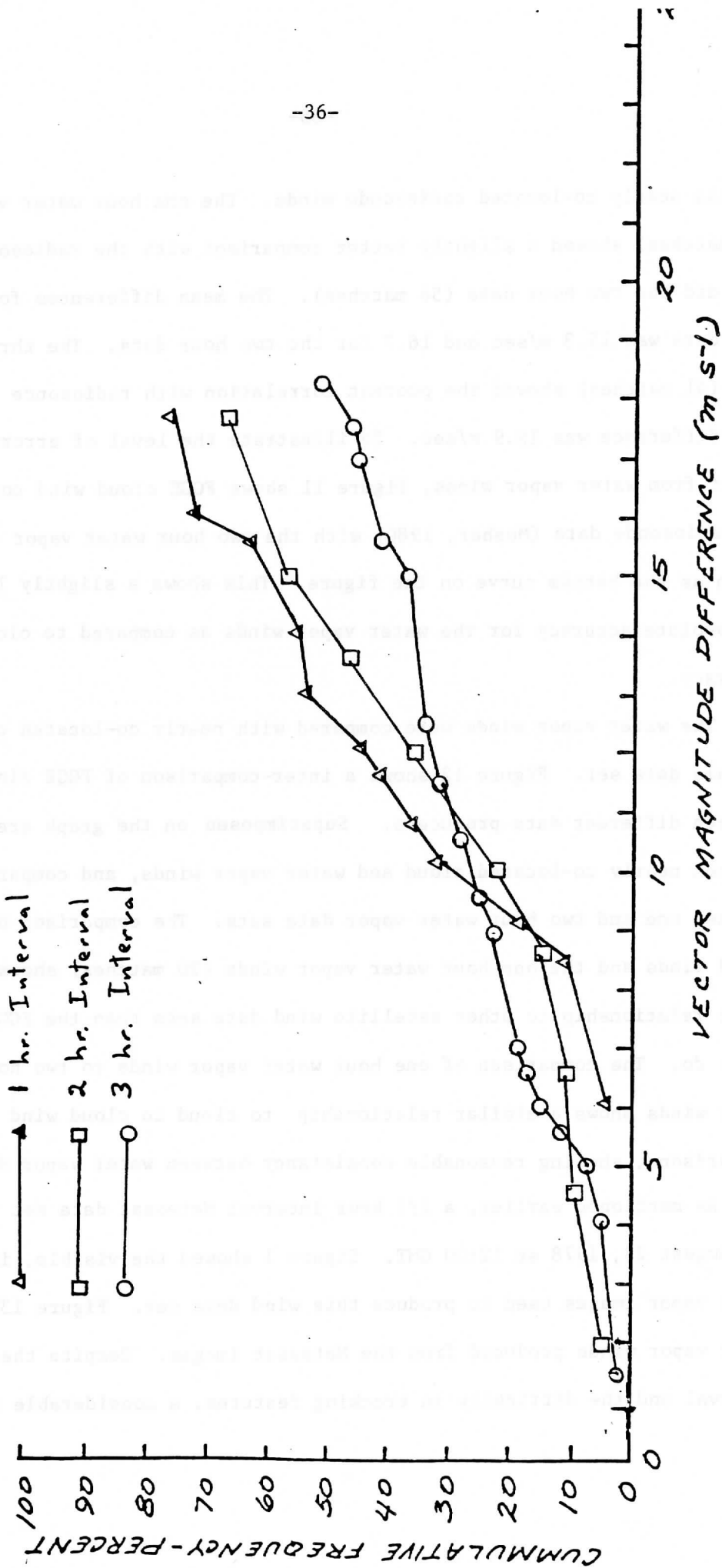
-36-

Figure 10. Cummulative frequency (percent) of the vector magnitude differences between water vapor winds and nearly co-located radiosonde winds.
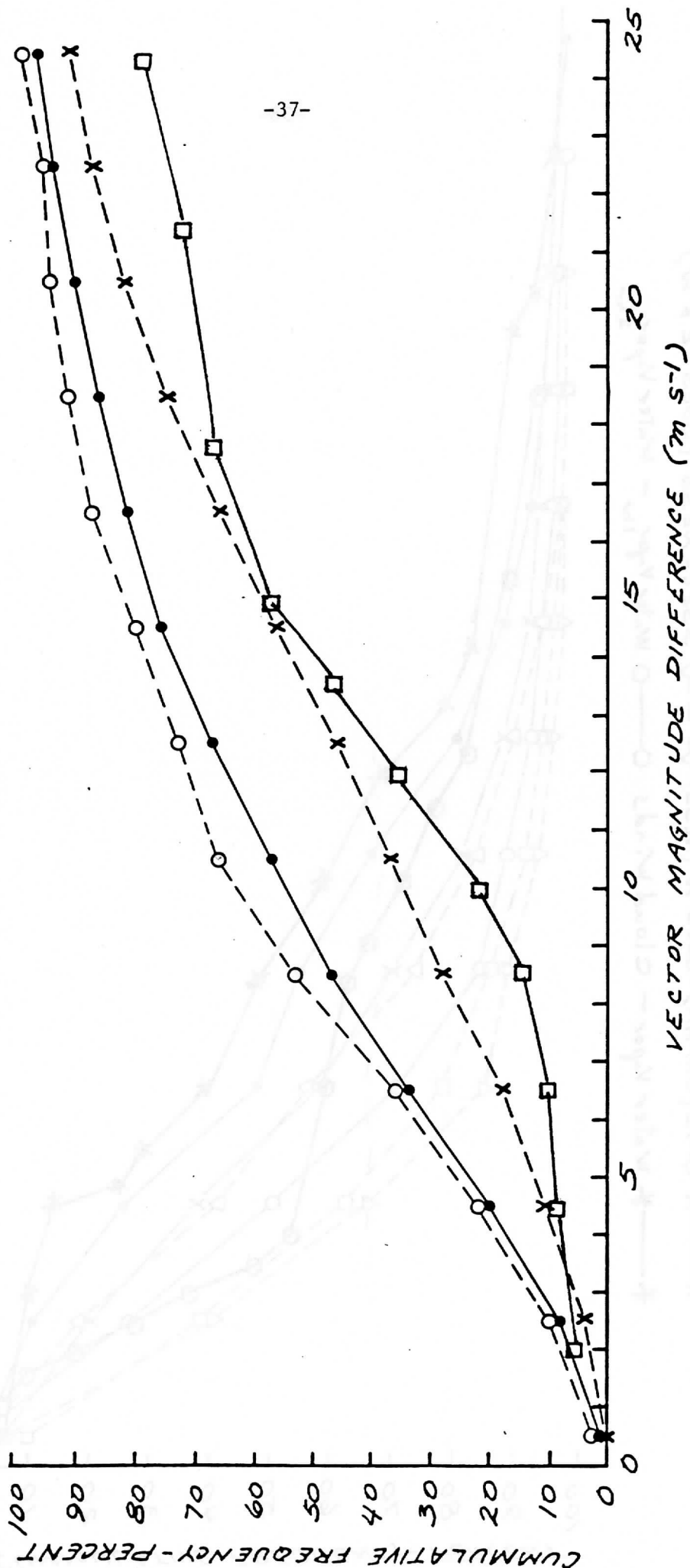
Figure 11. Comparison of FGGE cloud winds with radiosonde ground truth and the comparison of the two hour water vapor winds with radiosonde ground truth.
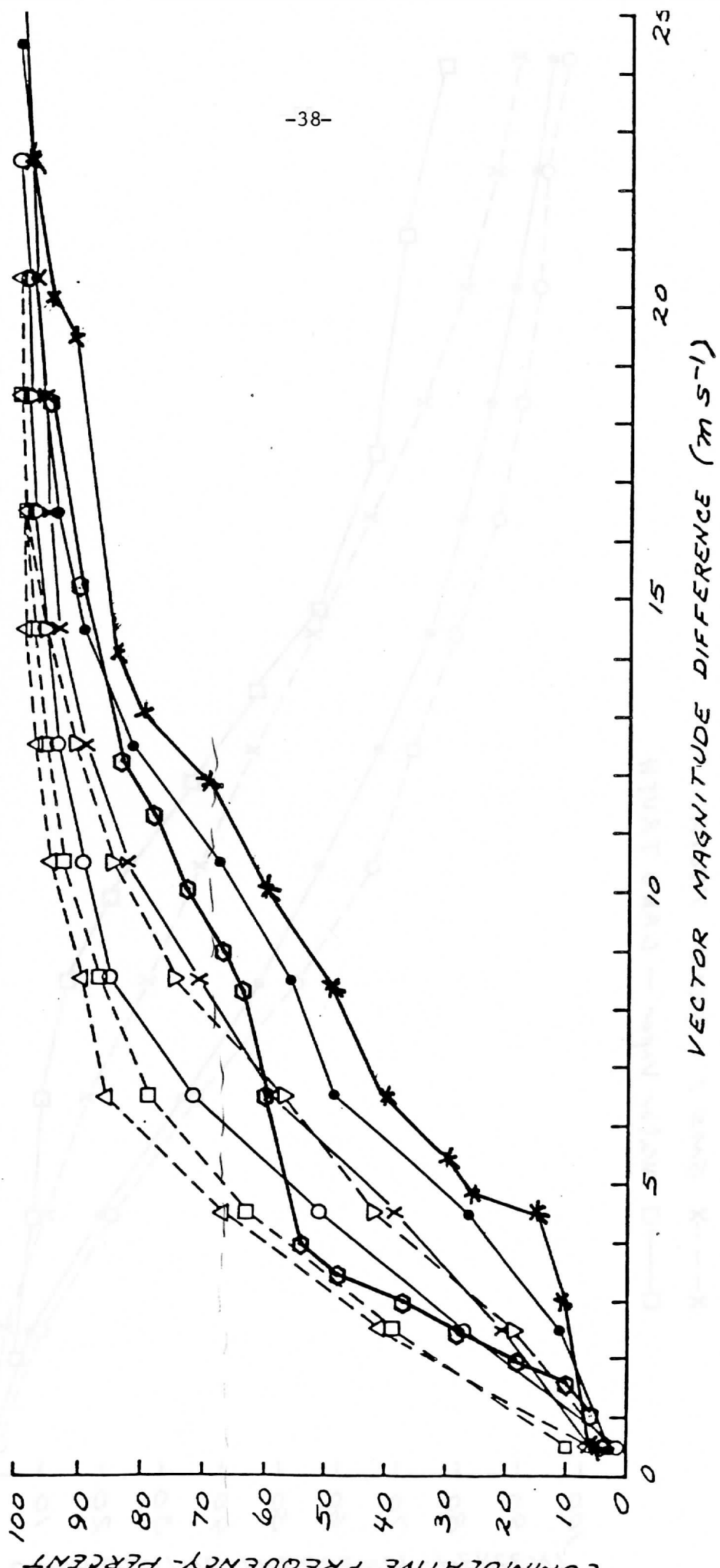
Figure 12. Intercomparison of FGGE cloud winds between different data producers, the comparison of water vapor winds with cloud winds, and the intercomparison of water vapor wind sets with different image time intervals.

vectors were derived. A total of 354 winds were produced on the Meteosat
images as opposed to 131 winds from the VAS data. This is primarily due to
the different spacial resolutions of the instruments. The Meteosat had a
resolution of 5 km while the VAS had a resolution of 14 km. The VAS resolution
was further degraded by the loss of one of the IR sensors which resulted in
every other line being missing, and was filled with the average of the data
on either side. Hence the north-south resolution of the VAS was approximately
28 km. The higher resolution of the Meteosat allowed more features to be
defined and tracked.

Figure 14a shows the high-level cloud tracked winds, figure 14b shows
the mid-level cloud wind, and figure 14c shows the low-level cloud winds.
Figure 15a shows the high-level combined water vapor and cloud wind data set.
The water vapor data was able to provide a few additional high-level winds.
The combined mid-level data set is shown in figure 15b. Here, most of the
vectors were derived from the water vapor data. There are a sufficient number
to provide a good mid-level analysis, something which generally is not
available from cloud winds alone.

VI. Conclusions

It is possible to obtain wind measurements in clear air remotely from
satellites by tracking water vapor in homogeneities. The 6.7 micron water
vapor channel on the Meteosat and GOES-VAS satellites provide images which
can be used in processing systems equiped to track clouds. While the
pure water features are fuzzy, they are discernible features which can be
tracked. These features have horizontal dimensions on the order of 100 km
and lifetimes of up to six hours. We investigated various methods to
preprocess the water vapor images to help bring out the features to be
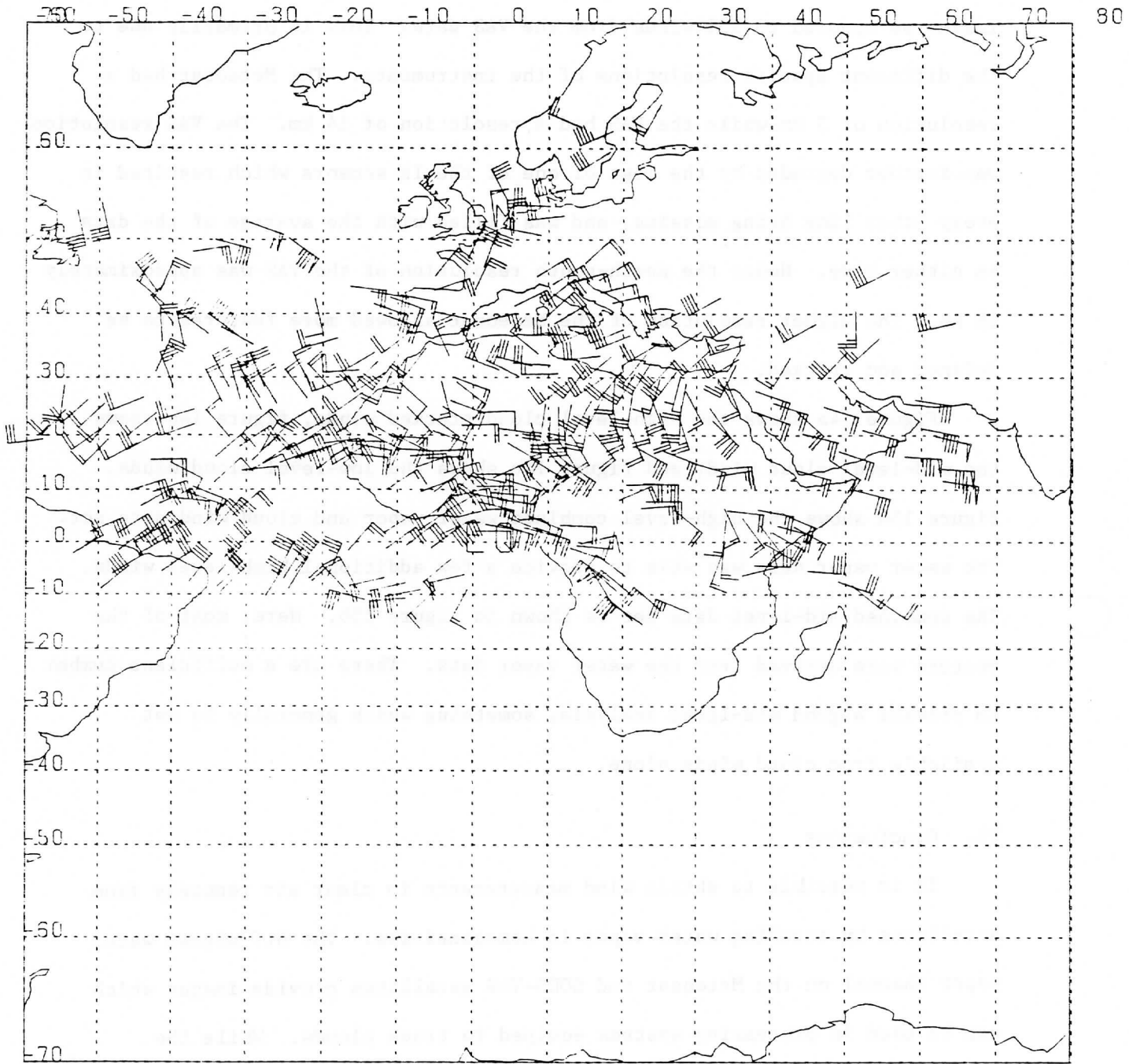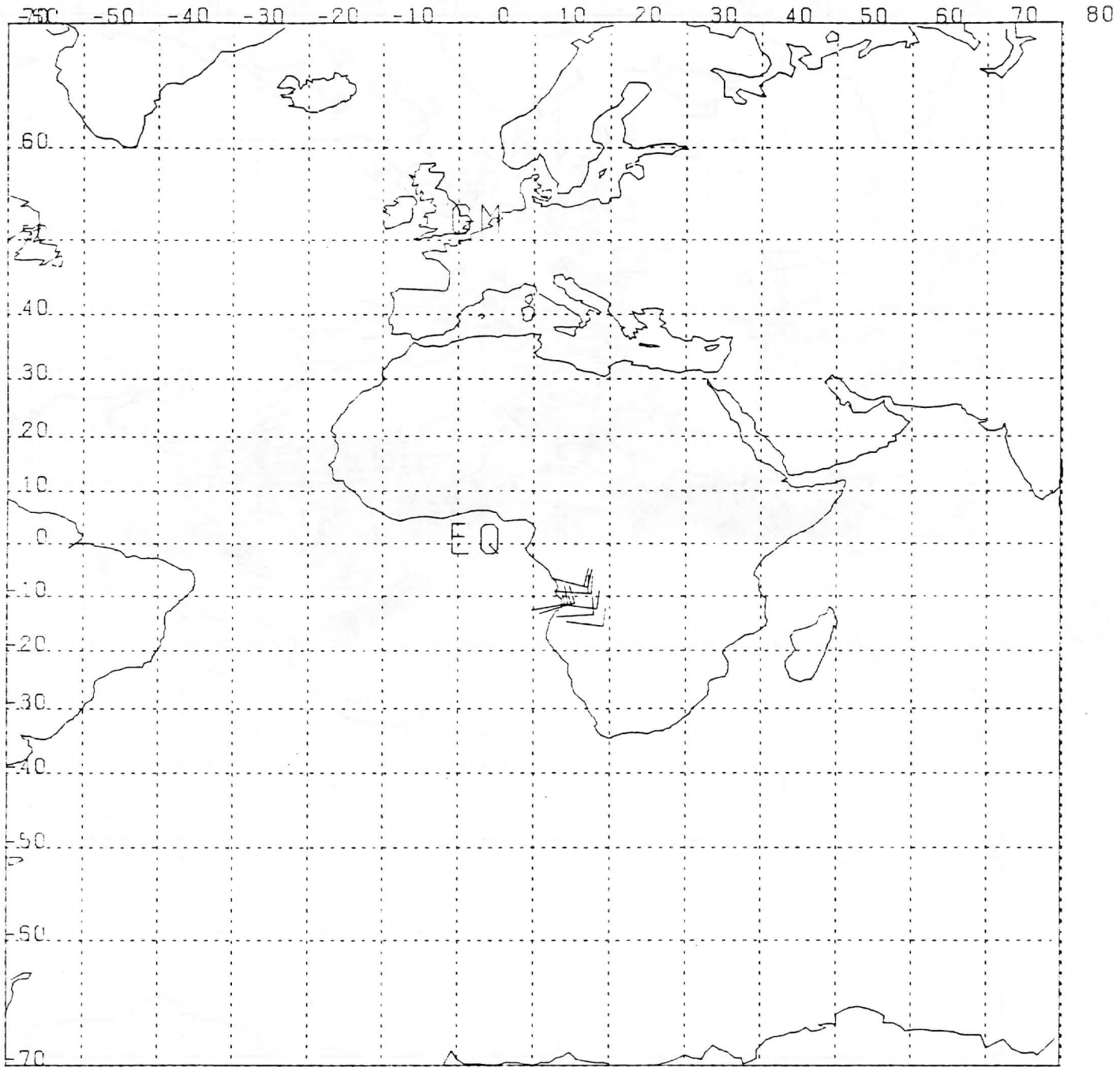
DAY 678235 TIME120249 500- 300 ME

Figure 13. Water vapor winds made from Meteosat images from August 23, 1978 at 12:00 GMT.
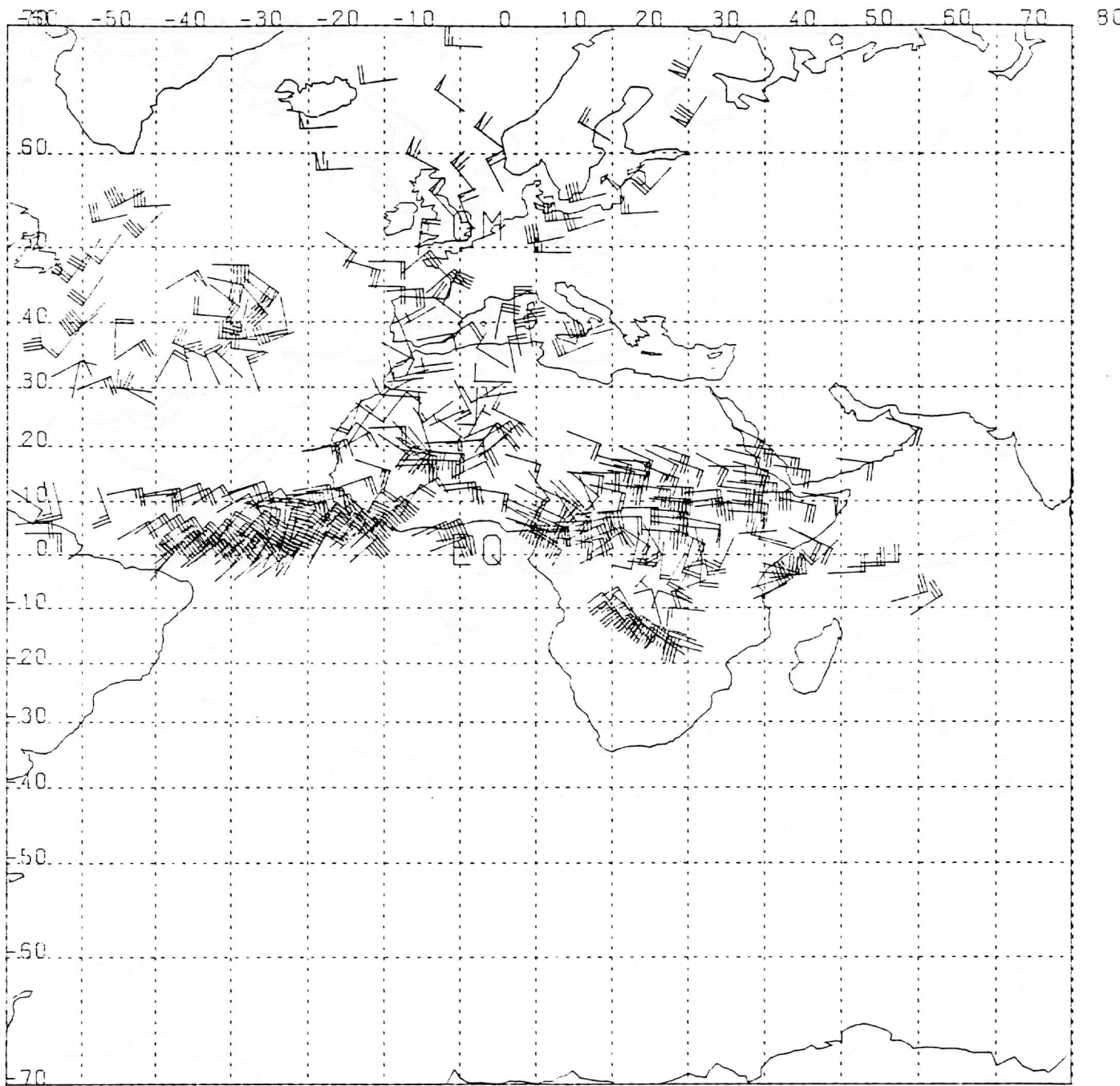
DAY 478235 TIME120249 350- 100 M

Figure 14a. High-level cloud winds from Meteosat images from
August 23, 1978 at 12:00 GMT.

DAY 478235 TIME120249 651- 350 MB

Figure 14b. Mid-level cloud tracked winds which correspond to Figure 14a.
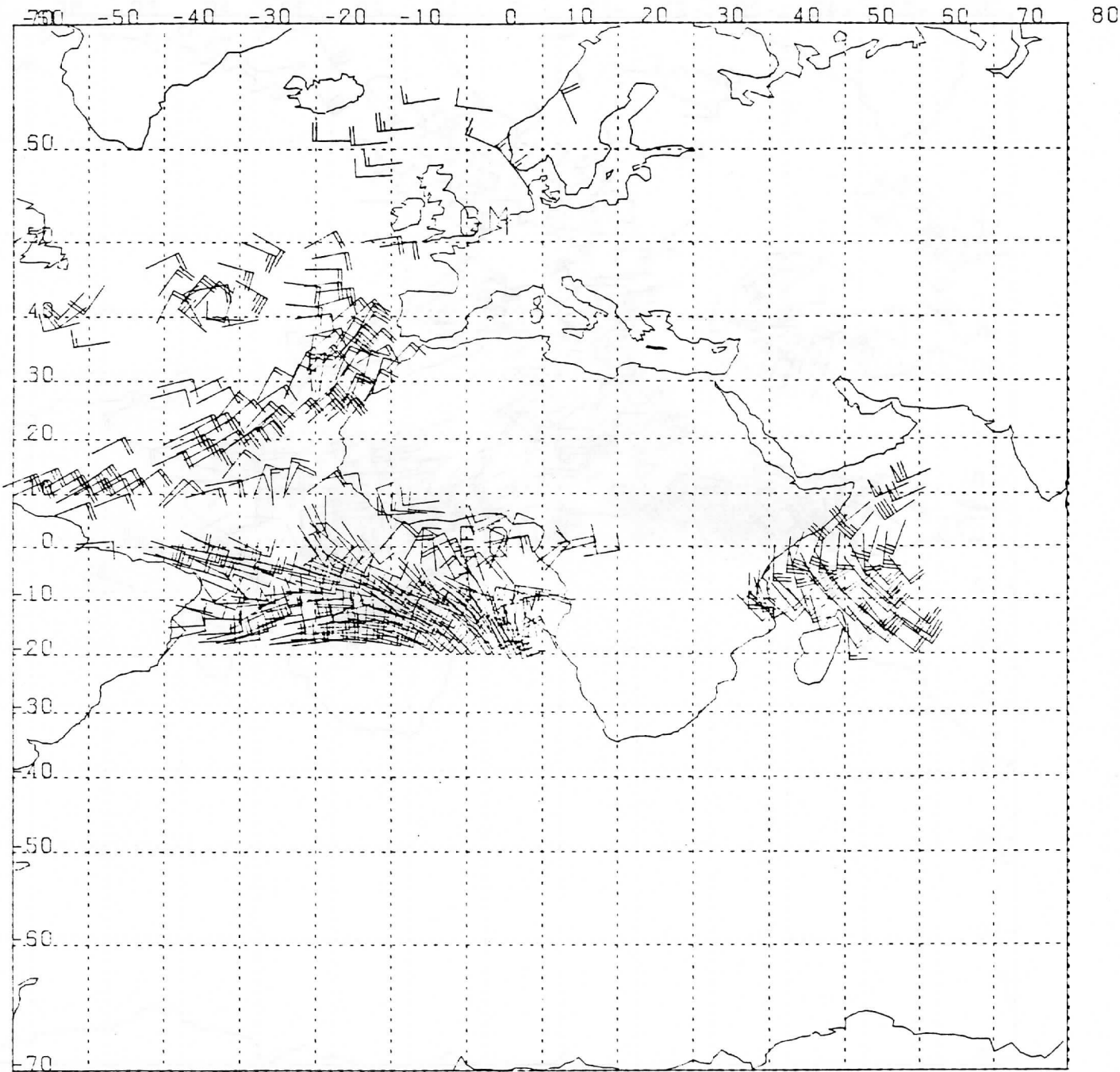
DAY 478235 TIME120249   999- 651 ME

Figure 14c. Low-level cloud winds which correspond to Figure 14a.
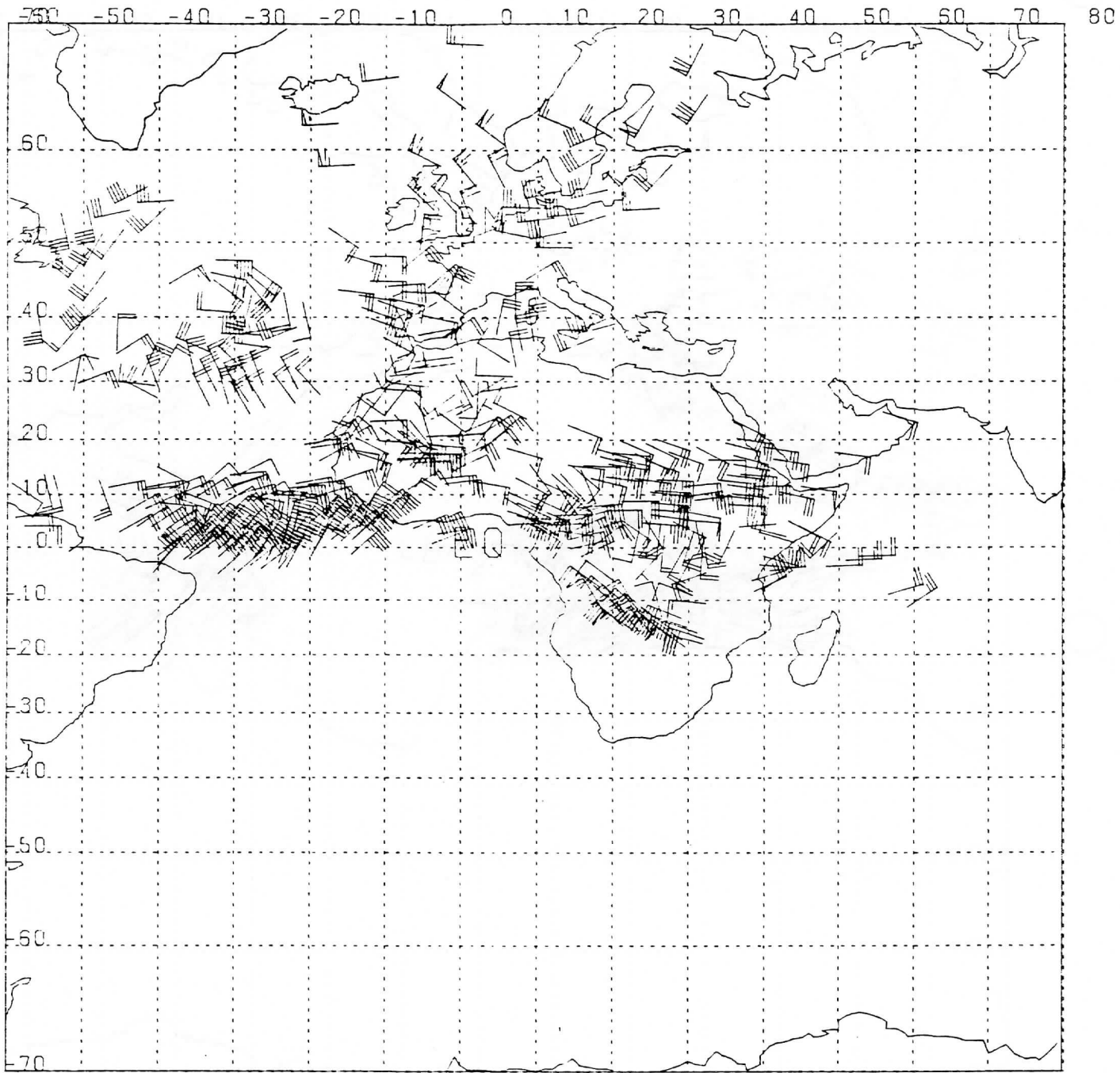
DAY 678235 TIME120249 350- 100 ME

Figure 15a. High-level combined cloud winds and water vapor winds
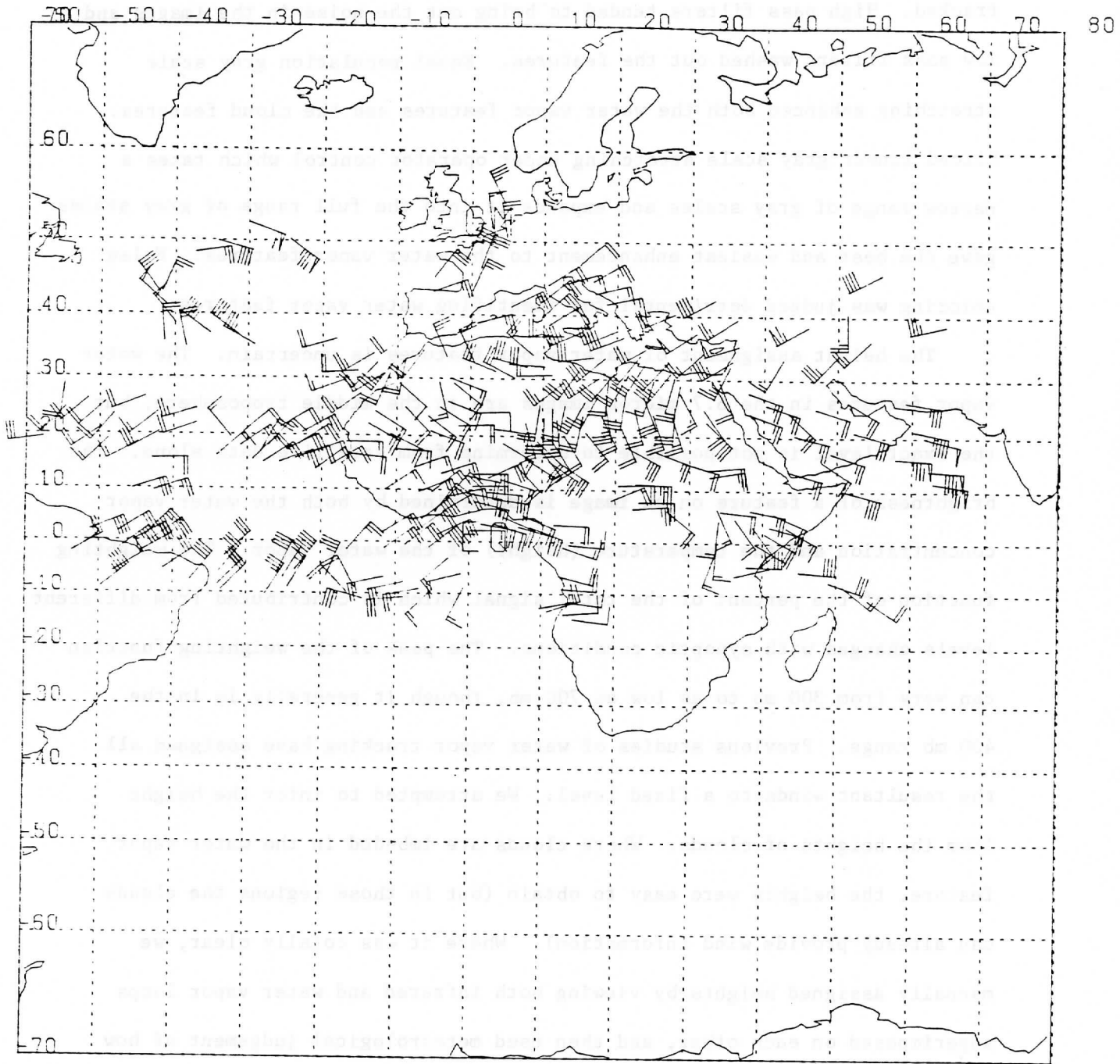for August 23, 1978 at 12:00 GMT.

DAY 678235 TIME120249 650- 351 MB

Figure 15b. Mid-level combined cloud winds and water vapor winds.
Almost all the information in the mid-levels is provided by the
water vapor winds.

tracked. High pass filters tended to bring out the noise in the images and low pass filters washed out the features. Equal population gray scale stretching enhanced both the water vapor features and the cloud features. Sliced linear gray scale stretching under operator control which takes a narrow range of gray scales and expands it into the full range of gray scales gave the best and easiest enhancement to the water vapor features. False coloring was judged detrimental for identifing water vapor features.

The height assignment of water vapor features is uncertain. The water vapor features in the 6.7 micron images are in the middle troposphere, but the exact level is not possible to determine from satellite data alone. The brightness of a feature on an image is determined by both the water vapor concentration and the temperature (height) of the water vapor. The weighting function of the percent of the total signal which is contributed from different levels changes with synoptic conditions. The peak of the weighting function can vary from 300 mb to as low as 700 mb, though it generally is in the 400 mb range. Previous studies of water vapor tracking have assigned all the resultant winds to a fixed level. We attempted to infer the height from the heights of clouds. Where clouds are imbeded in the water vapor feature, the heights were easy to obtain (but in those regions the clouds can already provide wind information). Where it was totally clear, we manually assigned heights by viewing both infrared and water vapor loops superimposed on each other, and then used meteorological judgement of how synoptic systems should behave to assign the heights relative to the known flow patterns of the cloud. This approach was reasonably successful.

The water vapor tracking was done interactively on the McIDAS with three images in a loop. Correlation tracking was attempted, but was generally not

successful. Only about 10% of the water vapor measurements were made with computer correlation. The water vapor features were generally too fuzzy for the correlation. Manual tracking was used for the rest of the water vapor measurements. Because the water vapor features are poorly defined, it was difficult to track them with short time intervals between images. By using longer time intervals, the placement error of the beginning and ending location of the feature was minimized. Time intervals between one and two hours (for a three image loop this is a total tracking time of two to four hours) appear optimal between tracking ability and life time of the water vapor feature.

The spacial resolution of the image can also influence the ability to track water vapor. The Meteosat data with its 5 km resolution showed many more small scale features which could be tracked than did the VAS with it's 14 km (28 km in the north-south direction due to a failed sensor) resolution.

Analysis of the fields of water vapor and cloud tracked winds show that the water vapor winds do provide additional meteorological information, particularly around jet cores. The water vapor winds were able to define jet cores missed by the cloud tracking. The water vapor winds also provided mid-level information generally lacking with cloud wind data. On the minus side, there still are a few clear areas which do not have any water vapor features, so no winds are available in those regions.

Comparisons of the water vapor winds with radiosonde and cloud wind data show that water vapor winds have a slightly lower quality than cloud winds. The error trends of the water vapor winds are the same as the cloud winds, only slightly worse by about 2m/sec. This is probably due to the difficulty in tracking caused by the fuzzy appearance of the water vapor features and to

the uncertainty of the height assignment.

In summary, water vapor tracked winds to provide valuable wind infor-
mation in clear areas and mid-levels and will contribute toward a more
complete satellite cloud tracked wind data set. The errors associated
with water vapor tracking are slightly worse than those associated with
cloud tracked winds. Water vapor images are available from the Meteosat,
and the VAS instruments on GOES-east and west. This water vapor data
should be used to obtain winds, but the search for better ways to remotely
sense winds in clear air should continue to be pursued.

REFERENCES

Allison, Lewis, J., Joseph Sterenka, C. Thomas Cherrix, and Ernest Hilsenrath

Bauer, Ernest, 1974: Dispersion of tracers in the atmosphere and ocean: Survey and comparison of experimental data. Journal of Geophysical Research, Vol. 79, No. 6, 789-795

Eigenwillig, Norbert, and Herbert Fischei, 1981: Determination of mid tropospheric wind vectors by tracking pure water vapor structures in Meteosat water vapor images. Submitted to the Bulletin of the American Meteorological Society

Endlich, Roy M., and Daniel E. Wolf; 1981: Automatic cloud tracking applied to GOES and METEOSAT observations. Journal of Applied Meteorology, 20, 309-319

Hinton, B. B., 1977: Climatology based on winds derived from cloud motions. Studies of soundings and imaging measurements, Final Scientific Report on NAS5-24136, Space Science and Engineering Center, University of Wisconsin-Madison, 231-273.

Johnson, Larry R.; 1980: Global winds, by tracking Meteosat water vapor pattersn. Studies of the Atmosphere Using Aerospace Probes. Scientific Report on NOAA Grant 04-L-158-44087, Space Science and Engineering Center, University of Wisconsin-Madison. 132-154.

Kästmer. Martina. Herbert Fischer, and Hans-Jürgen Bolle; 1980: Wind determination from Nimbus 5 observations in the 6.3 μm water vapor bind. Journal of Applied Meteorology, Vol 19, No. 4, 409-418.

Morel, Pierre, 1978: A new insight into the toposphere with the water vapor channel of Meteosat. Bulletin of the American Meteorological Society, 59, 711-714

Mosher, F. R., 1977: Feasibility of using water vapor as a tracer to obtain winds from satellite observations. Studies of Soundings and Imaging Measurements, Final Scientific Report on NAS5-24136, Space Science and Engineering Center, University of Wisconsin-Madison, 171-176.

Mosher, F. R., 1979: Cloud drift winds from geostationary satellites. Atmospheric Technology, 10, National Center for Atmospheric Research, CO, 53-60

Mosher, F. R., 1980: The compatability of cloud tracked winds from the United States, Europena, and Japanese geostationary satellites. Adv. Space Res., Vol. 1, pp 139-146.

Rossby, C. G. and Collaborators, 1937: Isentropic analysis, Bulletin of the American Meteorological Society, pp. 201-209

Smith, W. L., et. al, 1981: First soinding results from VAS-D. Bulletin of the American Meteorological Society, 62, 323-236.

Steranka, Joseph, Lewis J. Allison, and Vincent V. Salomonson, "Application of Nimbus 4 THIR 6.7 m Observations to regional and Global Moisture and Wind Field Analysis," Journal of Applied Meteorology, 12, pp. 386-395, March 1973.